In presenting the dissertation as a partial fulfillment of the requirements for an advanced degree from the Georgia Institute of Technology, I agree that the Library of the Institution shall make it available for inspection and circulation in accordance with its regulations governing materials of this type. I agree that permission to copy from, or to publish from, this dissertation may be granted by the professor under whose direction it was written, or, in his absence, by the Dean of the Graduate Division when such copying or publication is solely for scholarly purposes and does not involve potential financial gain. It is understood that any copying from, or publication of, this dissertation which involves potential financial gain will not be allowed without written permission.

_____

_____

A STUDY OF THE FRACTURE MECHANISM OF THREE ALUMINUM - COPPER ALLOYS IN THE REGION OF THE SOLIDUS

A THESIS

Presented to

The Faculty of the Graduate Division

by

James Frederick Crondin

In Partial Fulfillment of

the Requirements for the Degree of

Master of Science in

Mechanical Engineering

Georgia Institute of Technology

February, 1965

A STUDY OF THE FRACTURE MECHANIAM

OF THREE ALUMINUM - COPPER ALLOYS

IN THE REGION OF THE SOLIDUS

Approved:

Date Approved by Chairman: Feb. 5, 1965

ACKNOWLEDGMENTS

The author would like to express his thanks to Dr. Thomas F. Talbot, who suggested this research topic and served as his advisor. Thanks are also extended to Dr. John Bailey and to Dr. Robert Hochman for serving on the reading committee.

This work was supported by a National Science Foundation Research Grant.

TABLE OF CONTENTS

TABLE OF CONTENTS (Continued)

LIST OF TABLES

LIST OF ILLUSTRATIONS

LIST OF ILLUSTRATIONS (Continued)

LIST OF ILLUSTRATIONS (Continued)

SUMMARY

An experimental investigation of the fracture mechanism of three aluminum-copper alloys in the region of the solidus temperature has been carried out. The specimens used in this investigation were machined from extruded rods that contained nominal copper contents of two, four and six per cent. Each specimen was placed in a vacuum capsule, heated to the test temperature, and loaded to fracture in tension in an Instron Tensile Testing Instrument. Strain rates of 0.02, 0.20, 1.0 and 20.0 inches per minute were used in conducting the investigation. After fracture the specimens were rapidly cooled and then examined both microscopically and macroscopically.

The results of the investigation showed that as the temperature was increased the strength of the aluminum-copper alloys decreased rapidly to relatively low values at the solidus temperature. Above the solidus the alloys had practically no strength. Also the ductility of the aluminum-copper alloys increased as the temperature was increased until it reached a maximum at about 20 to 50 (usually about 50) degrees centigrade below the solidus of each alloy. Then it decreased to small values as the temperature approached the solidus.

An increase in the strain rate resulted in an increase in the strength of the alloys below the solidus. Above the solidus the strength fell off more quickly for higher strain rates than for the lower strain rates. An increase in the strain rate also decreased the ductility of the alloys.

There were three types of fracture that occurred in the aluminum-copper alloy system when tested in the region of the solidus. The first type occurred below the solidus and consisted of plastic deformation. The second type occurred within plus or minus a few degrees of the solidus. It consisted of both plastic deformation and intergranular failure. The third type occurred above the solidus and consisted entirely of grain boundary separation.

The ductile fracture was accompanied by large elongations and, at temperatures around 200 to 250 degrees centigrade, typical cup-and-cone fracture. At temperatures above about 300 degrees centigrade the specimens generally necked down to a point before fracture. The second type of fracture was accompanied by a small amount of elongation, but the fracture area consisted mainly of intergranular brittle type failure. Some of the area on the grain surfaces was rough, indicating solid-to-solid contact between some of the grains. In the third type of fracture there was very little elongation, and as the temperature increased above the solidus the rough fracture area disappeared. The fracture surface became completely smooth, and the type of fracture consisted entirely of grain boundary separation.

Specimens tested at elevated temperatures exhibited a relatively uniform reduction in area along the entire length of the specimen even after the maximum load had been attained. This uniform elongation is in contradiction to what is known concerning the behavior of tension-test bars at low temperatures, in which localized necking sets in right after the maximum load is reached. It is proposed that the uniform

elongation results from a combination of the work hardening, recovery, and recrystallization processes.

CHAPTER I

INTRODUCTION

Statement of Intent

The intent of this experimental investigation is to study the fracture mechanism of three aluminum-copper alloys in the region of and below the solidus temperature. The results of this investigation will be used to help develop a better understanding of the deformation of aluminum-copper alloys at elevated temperatures up to and including the solidus.

Application of This Type of Research

For many years metallurgists have been interested in and studying the physical and mechanical properties of alloys in the region of the solidus. Of prime interest has been the cause and elimination of hot-tearing, hot-cracking and hot-shortness of materials during casting, welding and hot forming operations. However, much of the research work in this area has not taken into consideration the mechanisms involved. The work that has been done was primarily concerned with casting failures, and therefore the problem was approached from the view of the foundryman and development of casting techniques.

A further development of conventional casting is the continuous casting process, which has many advantages over the conventional casting method. Several of the more important ones are elimination of metal

losses, improvement of cast structure, and the reduction of labor requirements. However, there are many problems in this process that still must be solved. Also, a continuation of the continuous casting process is the integration of this method into a continuous casting and rolling mill which would save substantial energy and manpower. Before this can be completely accomplished successfully, many questions about the basic mechanism of the physical occurrences during the casting and rolling operations will have to be answered and understood more thoroughly. It is the purpose of this research to help answer some of these questions.

At present there are a limited number of continuous casting-rolling mills in operation, and they are mostly in England and Russia. However, many problems are being experienced by these mills. An even further development is extrusion casting, where metals and alloys may be fabricated during solidification.

So it can be seen that there is a great need for a better understanding of metals and their properties in the temperature range of the solidus. Most of the research in this area has been concerned with the hot-tearing of castings and welds, and this is the basis for this investigation.

Historical Background

There has been much information published concerning the cracking of metals in the temperature range of the solidus; however, only the articles of major importance will be discussed. There are several different types of tests, and each of these will be discussed separately.

Cracking Caused by Shrinkage in Casting Tests

Casting of various shapes were made to produce various amounts of strain. Singer and Jennings[1] made castings of alloys of commercial purity aluminum-silicon in an annular mold in which stresses were set up by contraction during cooling. The severity of cracking was found to be related to the mechanical properties of the alloys at high temperatures.

Jennings, Singer, and Pumphrey[2] carried out ring-casting tests on alloys of high-purity aluminum-copper-silicon and aluminum-magnesium-silicon. The results enabled them to extend the original hot-shortness theory for binary systems to ternary systems.

Prokhorov[3] designed a new type of casting to measure the resistance of metals to hot-tearing. It consisted of two V-shaped bars connected by a series of parallel bars of gradually increasing length. The parallel bars of different lengths constituted the test specimens. The metal at the junctions was the last to solidify, so therefore the strain was concentrated in that region. However, no significant results were obtained from this test.

The main disadvantage of the casting test is that the data from different types of casting tests cannot be correlated.

Impact Tests

Eborall and Gregory[4] performed the most significant impact tests using specimens made of lead-beta brass and lead-bronze. The specimens were heated to temperatures just above the solidus before the tensile-impact tests were performed. They found that the presence of liquid lead resulted in brittle fracture with grain boundary failure, but that

the liquid did not spread around the boundaries in the absence of stress. Failure was accompanied by the spreading of the liquid lead over the fracture surface.

According to the Griffith[5] theory of cracking, the stress needed to make a given crack grow depends on the surface energy required to form fresh surfaces. Eborall and Gregory believed that this stress needed to make a crack grow could be greatly reduced if the tip of the crack were filled with the liquid phase. This is in agreement with C. S. Smith[6] who predicted that the liquid phase, for small values of the included angle, spreads under stress and that the spreading of the liquid should take place at stresses much below those needed for the growth of a crack containing no liquid.

The main disadvantage of this type of test is that they are difficult to control. To date no useful general theory has been advanced from these tests.

Bend Tests

At temperatures approaching the solidus it was found by Vero[7] that the bending strength of an aluminum-silicon alloy decreased. He also found that the strength of some alloys, such as aluminum-silicon, fell rapidly to zero at the solidus while the strength of other alloys decreased gradually as the temperature increased. However, Vero abandoned this research when he was unable to formulate any theory from the results.

Tensile Tests on Prepared Specimens

To date the most important contributions in the area of hot-shortness have been obtained from tensile tests on prepared specimens.

Vero[7] was one of the first investigators to perform these tests. However, he was unable to explain his results, and he abandoned these tests in favor of the bend tests described in the previous section.

Singer and Cottrell[8] performed tensile tests on aluminum-silicon alloys at temperatures in the region of the solidus to obtain information that would assist in explaining the mechanism of hot-shortness. They found that up to the solidus temperature the elongation and reduction of area of all alloys remained high, but that at and above the solidus temperature elongation and reduction of area approached zero and the strength rapidly decreased to a very low value. The coherency of the alloy was determined to be dependent on the temperature and the chemical composition. By microscopic investigation it was possible to link the tensile properties at temperatures in the region of the solidus with the aluminum-silicon equilibrium diagram. They also concluded that the extent of the temperature range above the solidus over which the alloys possess a finite strength yet have no appreciable ductility may be one of the principal factors determining their hot-shortness characteristics.

Pumphrey and Jennings[9] repeated the tests of Singer and Cottrell except that instead of an equilibrium alloy they used a chill cast alloy that had been rapidly reheated to assure non-equilibrium conditions. The results were similar to those of Singer and Cottrell except that the temperature of embrittlement varied. This was to be expected because of the non-equilibrium condition of the alloys.

Lyons and Pumphrey[10] repeated the experiments of Singer and Cottrell using aluminum-copper, aluminum-iron, aluminum-manganese, and aluminum-zinc alloys in the cast condition. They found that surface

cracks existed at points other than in the area of failure and that the grain boundaries melted at a temperature slightly below the melting point of the metal. This latter point was thought to be caused by the high strain energy in the boundary regions.

Novikov[11] performed tensile tests on machined testpieces and stated that the elongation suddenly dropped on passing through the solidus to very low values. This sudden drop in elongation at the solidus was thought to be caused by the major decrease in shear strength at the macrograin boundaries as a result of grain boundary fusion.

Talbot[12] performed tensile tests using specimens machined from aluminum-copper alloys. His results showed that the tensile strength fell off sharply at the solidus temperature and that the elongation was greatest about 50 degrees centigrade below the solidus. Also it was shown that an increase in strain rate increased the tensile strength in the region below the solidus.

Nadai and Manjoine[13] performed experiments on prepared tensile specimens to investigate the resistance to plastic forming of several metals over a wide range of rates of deformation at various temperatures. The general trend of their test results for aluminum and copper indicated a continuous increase of the yield stress with increasing strain rate. They found that at very rapid rates of deformation the ultimate stresses were remarkably high for aluminum and copper when tested at temperatures approaching their melting points.

Tensile Tests on Castings During Solidification

For many years this was the main method of investigation. However, results vary from investigation to investigation and have not been very

useful. This type of test is performed as the metal is solidifying (cooling) rather than heating a metal up to the desired temperature.

Pumphrey and Jennings[9] performed tensile tests on aluminum-silicon alloys during solidification. Their results verified what had been obtained earlier by Singer and Cottrell. The only difference was that they used a non-equilibrium alloy which changed the temperatures from those used by Singer and Cottrell.

Pellini[14] performed tensile tests using ferrous castings. He found that a liquid film is developed in a narrow temperature range at the solidus and that the strength and ductility of a metal which is being heated slowly drops to essentially zero over this range. This is in general agreement with other investigators.

The main disadvantage of the tensile tests on solidifying castings is that a solid shell which adds to the strength of the specimens exists, thereby not giving a true value for the strength of the specimen with liquid in it. Also there is an unknown temperature gradient in both the horizontal and vertical directions.

Weld Tests

Weld tests are included in this discussion only because cracks similar to the cracks in castings occur in welds under the same temperature conditions. Therefore it is believed that the mechanism is the same in both cases. However, the results of weld tests have been of very little value.

Singer and Jennings[1] carried out welding experiments along with casting tests on aluminum-silicon alloys of commercial purity and from the results were able to relate the hot-shortness theories for castings

to welds also. It was shown that there was a relationship between the cracking and the mechanical properties of the alloy at high temperatures.

Singer and Jennings[15] also performed welding tests using high-purity aluminum-silicon alloys with the addition of a third element, iron. The addition of iron was determined to delay and reduce the severity of cracing, but no theoretical reason was given for this effect. It was also noted that the silicon content should not exceed the iron content when commercially pure aluminum is to be cast or welded in conditions where contraction stresses may arise.

Jennings, Singer and Pumphrey[2] performed weld tests on high-purity alloys of aluminum-copper-silicon and aluminum-magnesium-silicon and found that the reasons for hot-shortness seemed to be constitutional. This was also found previously to be true for binary aluminum-silicon alloys. The original hot-shortness theory was then extended to ternary systems. They noted that its application was less straightforward, particularly in aluminum-magnesium-silicon alloys in which the presence of the Mg_2Si phase was a complicating factor.

Current Theories

There have been many theories proposed concerning hot-shortness, and some of the important ones will be discussed briefly here to give an indication of the ideas that are most prevalent. No one theory has been proved or accepted as absolutely correct, as evidenced by Borland[16] when he stated:

> There remains much work to do in attempting to verify the generalized theory and put it on a much more quantitative basis - if indeed this can be done - and in particular to correlate the physical properties of alloys with their known cracking susceptibilities.

Shrinkage-Brittleness Theory

This theory was the one believed by many of the early workers. It stated that cracking occurred only while the casting cooled through the brittle-temperature range, a temperature range related to the phase diagram. Essentially, there were four temperature ranges; (1) total liquid range, (2) range where dendrites form up to the stage of interlocking, (3) range where dendrites continue to grow and liquid channels contract preventing the flow of liquid, and (4) completely solid range. The third range was the one known as the brittle-temperature range.

Strain Theory

Pellini[14] suggested that hot cracking is caused by localized strains tending to pull apart solid masses of material that are separated by thin films of liquid. He stated that cracking can take place only when there is a liquid film separating the solid portions and when the localized strains are high.

Saveiko[17] also suggested a liquid-film theory in which the film is continuous across any section and the strain is concentrated in this area. He assumed that the fracture started in the film itself and proposed the following algebraic relationship:

$$P = \frac{2aF}{1000gb} \text{ kilograms}$$

where

P = Force to separate plates, kilograms

a = Surface tension of liquid, erg/cm^2

F = Area of contact between the plates and liquid, cm^2

b = Thickness of the liquid layer between the plates, cm

g = Gravitational acceleration, cm/sec^2

Liquid Crack Theory

Patterson[18] proposed this theory in which he applied the Griffith's crack theory to hot-shortness. He assumed that the crack filled with liquid and that this reduced the interfacial energies which, in turn, reduced the load required for failure.

Griffith's[5] crack theory states that in an elastic material the applied stress required to make a thin crack grow is

$$\sigma = (K\gamma_s)^{0.5}$$

where

σ = Stress

K = Proportionality constant

γ_s = Surface energy

Critical Speed Theory

Smolyanitsky[19] estimated that the probability of the formation of hot cracks in cooling castings was

$$P = \frac{Ve_{max}}{Ve_{crit}}$$

where

P = Probability of hot-shortness

Ve_{max} = Maximum actual speed of deformation of expansion of the metal

Ve_{crit} = Maximum speed of deformation at temperatures near the solidus

Borland's Generalized Theory

Borland[16] developed a generalized theory which is similar to the shrinkage-brittleness theory discussed earlier. The only difference is that he states cracking may occur in both the second and third temperature ranges, but that in the second range "liquid healing" may occur if the cracks do form. However, no "liquid healing" can occur in the third range if the "accommodation" strain is exceeded. "Accommodation" is the degree to which an alloy is able to withstand shrinkage strain by movement of the crystals within the semi-solid mass.

Grain-Boundary-Sliding Theory

Prokhorov[20] proposed this theory in which the grains rotate to allow deformation before brittle hot-shortness occurs. He assumed that the grains were surrounded by liquid and that failure occurred when the rotating grains became jammed. The jamming resulted in stresses being built up and finally cracks forming.

Purpose and Scope

The purpose of this thesis is to investigate the fracture mechanism of aluminum-copper alloys in the region of the solidus. The results will be used to try and give a better understanding of the physical processes that occur in this temperature region.

This work is a continuation of the investigation initiated by Dr. T. F. Talbot[12] in an effort to better understand the physical phenomenon of hot-shortness. It is also in conjunction with experimental work performed by J. H. Tundermann[21] in the same area.

CHAPTER II

APPARATUS

General

The apparatus used in the experimental research for this thesis can be divided into three sections. First, an Instron Tensile Testing Instrument was used to apply, measure and record the load applied to the specimens. Also, at the strain rate of 20.0 inches per minute a Tektronix oscilloscope with a polaroid camera attachment was used to record the applied load. Second, Instron High Temperature Tensile Testing Equipment was used to heat the specimens to the desired temperatures. The temperatures were measured using platinum-platinum ten per cent rhodium thermocouples and recorded with a Leeds and Northrup potentiometer. And third, a vacuum system composed of a Cenco Hyvac 14 Pump with suitable vacuum piping arrangement was used to create a vacuum in which the specimens were tested. The vacuum was measured with a portable thermocouple gauge control. After the specimens had been tested they were examined using a Bausch and Lomb StereoZoom Microscope, and photographs were taken using a stereo camera attachment. Then Instron Tensile Testing Instrument is shown in Figure 1 while the assembled apparatus is shown in Figure 2. A description of the individual components of the apparatus follows.

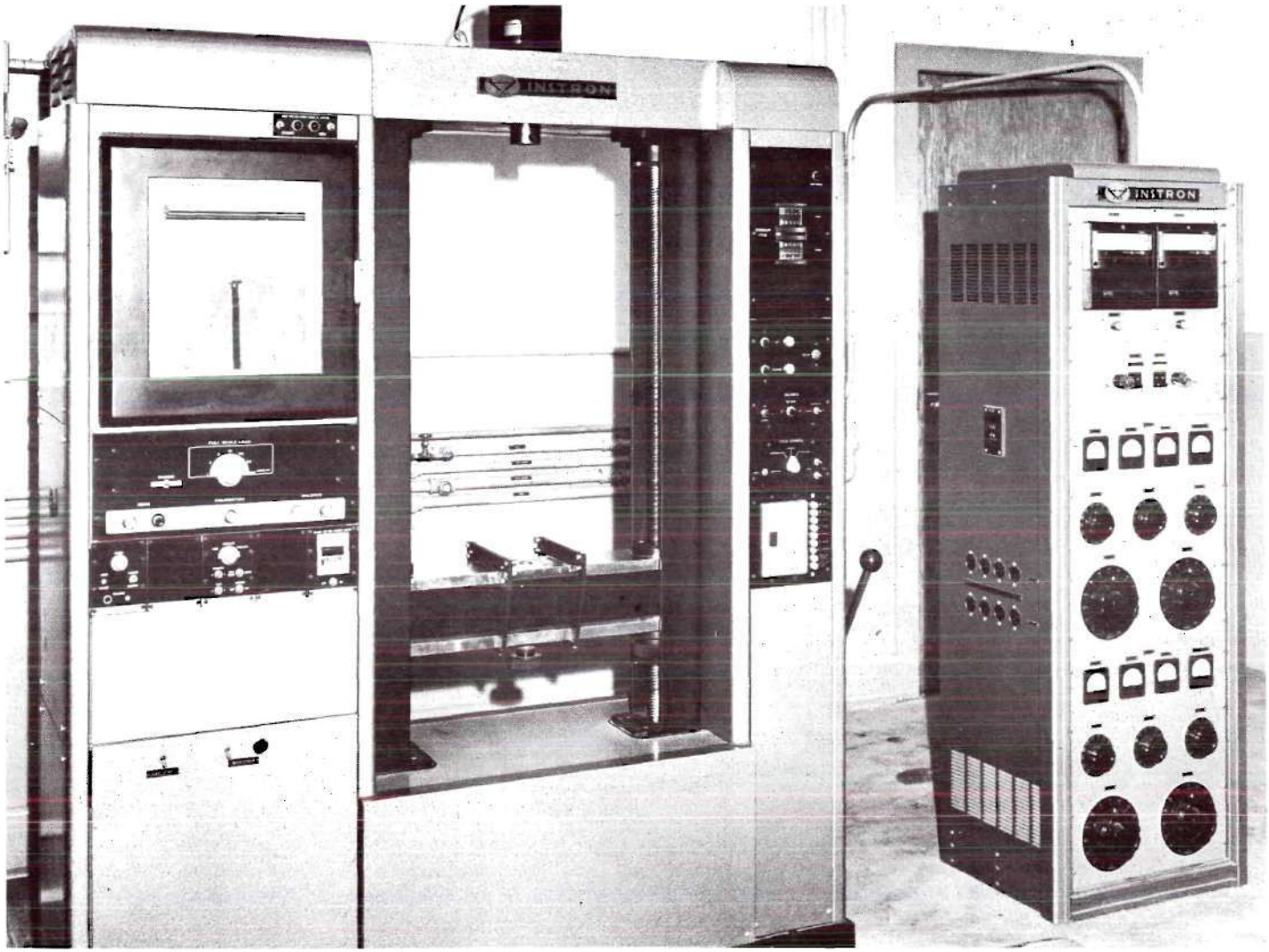

Figure 1. Instron Tensile Testing Instrument.

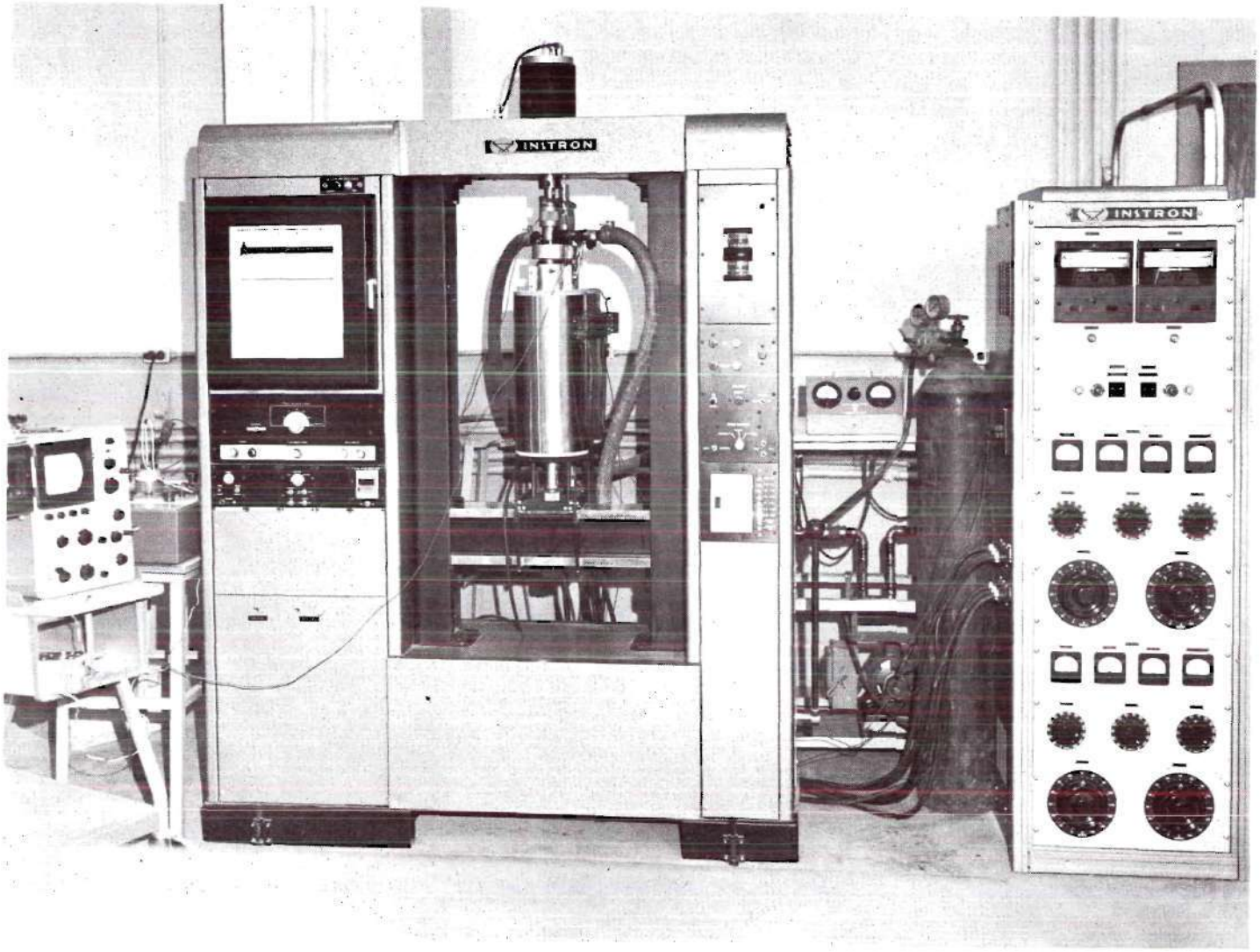

Figure 2. Experimental Equipment Arrangement

Components

Instron Tensile Testing Instrument

The Instron Tensile Testing Instrument as used for applying, measuring and recording loads contains three integral parts. They are the crosshead drive system, the load measuring system and the chart recorder and are described below.

Crosshead Drive System. Exact crosshead speeds over a range of 1000:1 in either direction of motion may be obtained through the operation of the servo-controlled drive. Crosshead speeds of 0.02, 0.05, 0.10, 0.12, 0.20, 0.50, 1.0, 1.2, 2.0, 5.0, 10, 12 and 20 inches per minute are provided by two vertical drive screws. Once selected, the crosshead speed remains constant for all of its rated loads.

Load Measuring System. The load measuring system consists of removable load cells which are inserted into the upper, fixed crosshead. The load cell used in the experimentation for this thesis had a maximum load range of 1000 pounds for full scale deflection on the chart recorder. A selector switch also allowed the sensitivity of this load cell to be increased to 500, 200, 100, 50, or 20 pounds full scale. In the load cell used, the load was measured using a strain sensitive member consisting of a simple tension bar with the wire resistance strain gauges applied to an area of reduced cross section. The gauges are connected in the form of a simple Wheatstone Bridge and are energized by a constant AC voltage from the machine. Application of a load causes the bar to lengthen, and as a result, the resistance of the strain gauges changes. Then the out-of-balance voltage of the Wheatstone Bridge is amplified and fed to the chart recorder.

Chart Recorder. The chart recorder is a Leeds and Northrup High Speed Type G Speedomax Strip Chart Recorder. It provides a span step response of less than 0.4 seconds for full scale pen travel and operates with an accuracy of plus or minus 0.3 per cent of the electrical span or plus or minus 15 microvolts, whichever is greater. Although the chart of the recorder is driven independently with respect to the crosshead, it is synchronized with the crosshead. This allows the extension axis of the chart to be magnified or demagnified and used as a time axis to determine the elongation of the specimens.

Tektronix Oscilloscope and Camera

A type 502 Dual-Beam Tektronix oscilloscope was used to measure the loads when the 20.0 inches per minute strain rate was used. The oscilloscope was connected to the output of the recorder amplifier through a specially built amplifier. This second amplifier was required because the frequency response (200 microvolts per centimeter for a 100 kilocycle signal) of the oscilloscope was much greater than required for the maximum strain rates used in this work.

An oscilloscope polaroid camera attachment was used to record the data on film. The attachment consisted of an optical system which allowed the simultaneous viewing and recording of the data.

Instron High Temperature Tensile Testing Equipment

This equipment is designed to permit tests to be performed at temperatures from room temperature to 2200 degrees Fahrenheit in a vacuum or in an inert atmosphere. It consists of a dual furnace temperature controller, two furnaces on a sliding base, two pull assemblies, and two vacuum capsule units.

The temperature in each furnace can be regulated to plus or minus two degrees Fahrenheit by the furnace temperature controller. It is controlled by an ON-OFF type of controller whose input is the EMF generated at the control thermocouple, which is imbedded in the furnace near the windings. Temperature overshoot is minimized by a special anticipator which adds an auxiliary EMF output to the thermocouple controlling the furnace during the ON cycle. A temperature cycling of less than plus or minus two degrees Fahrenheit can be attained by proper adjustment of this anticipator. The furnace is heated with a high power during the ON cycle and with less power during the OFF cycle. Variacs are provided to permit proportioning the power to the three furnace zones. The variacs also permit setting the ratio of ON cycle power to OFF cycle power.

Each furnace has three zones of Kanthal windings on a refractory tube. Each zone has a separate variac control so that each can be set independent of the others. A thermocouple is inserted in the wall for controlling the temperature.

The pull assemblies are made of high strength high temperature materials. Split collars are used to grip the specimens whose dimensions are shown in Figure 3. The tensile capsule container is constructed of a corrosion-resistant alloy to withstand oxidation and prevent collapse during vacuum at high temperatures. The pull-rod is allowed to move through the container under vacuum by the use of static O-rings and polished surfaces.

Temperature Measuring System

The temperature measuring system consisted of platinum-platinum ten per cent rhodium thermocouples, platinum-platinum ten per cent

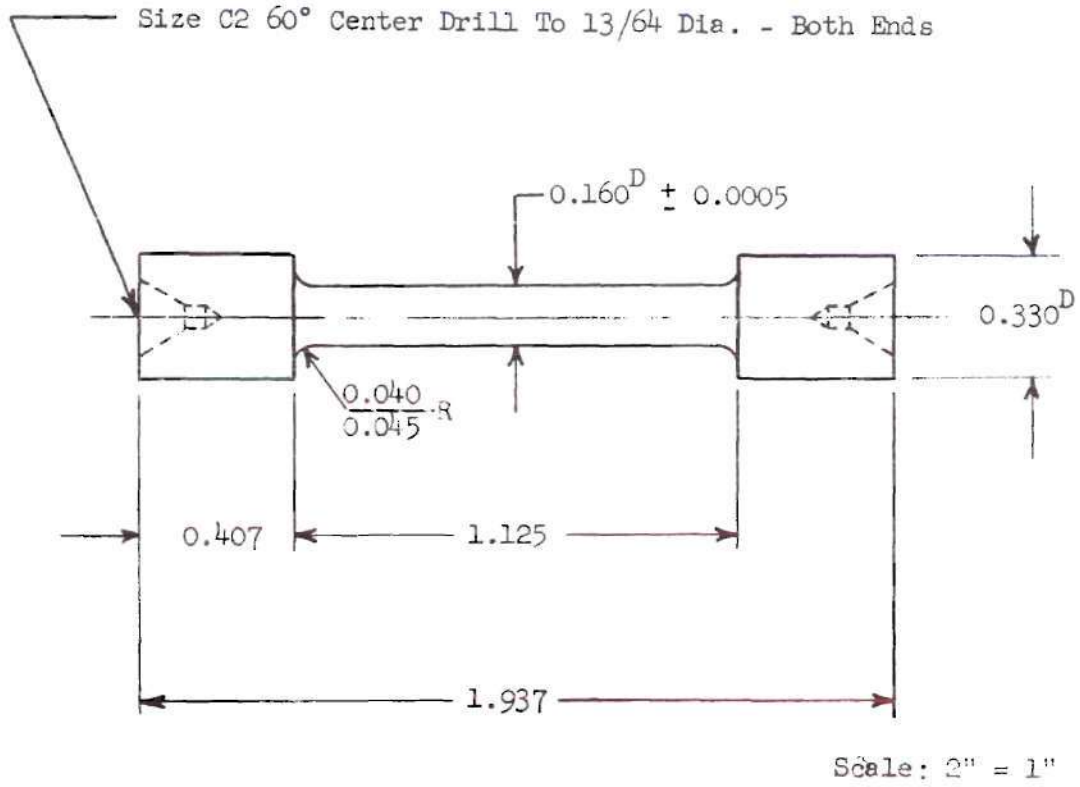

Figure 3. Tensile Test Specimen.

rhodium cold juntions, and a Leeds and Northrup millivolt potentiometer. The thermocouples were placed in the vacuum capsule near the test specimen, and the cold junctions were placed in an ice bath for the reference temperature. A schematic diagram of the thermocouple system is shown in Figure 4.

Calibration of the thermocouples indicated a repeatability of within plus 0.3 degrees centigrade of standard in the temperature range from 200 to 635 degrees centigrade. Details of the calibration are given in Appendix B.

Vacuum System

The vacuum system consisted of a Cenco Hyvac 14 Pump, a portable thermocouple gauge control and a suitable arrangement of vacuum piping and valves. The major components are described below.

Cenco Hyvac 14 Pump. This pump is a two-stage, series connected mechanical vacuum pump which has a guaranteed blank off vacuum of 0.1 microns of mercury and a capacity of 1.05 liters per second at one micron of mercury.

Portable Thermocouple Gauge Control. This gauge control will measure absolute pressure between 500 and two microns of mercury. It can also be used for leak detection at pressures of less than 200 microns of mercury. It is incorporated into the system through a thermocouple gauge which is screwed into a connection in the vacuum system.

Vacuum Piping Arrangement. The vacuum system showing the vacuum piping arrangement is illustrated in Figure 5. The valves and piping were arranged so that either one or both capsules could be evacuated at the same time, and also so that one or both capsules could be purged with

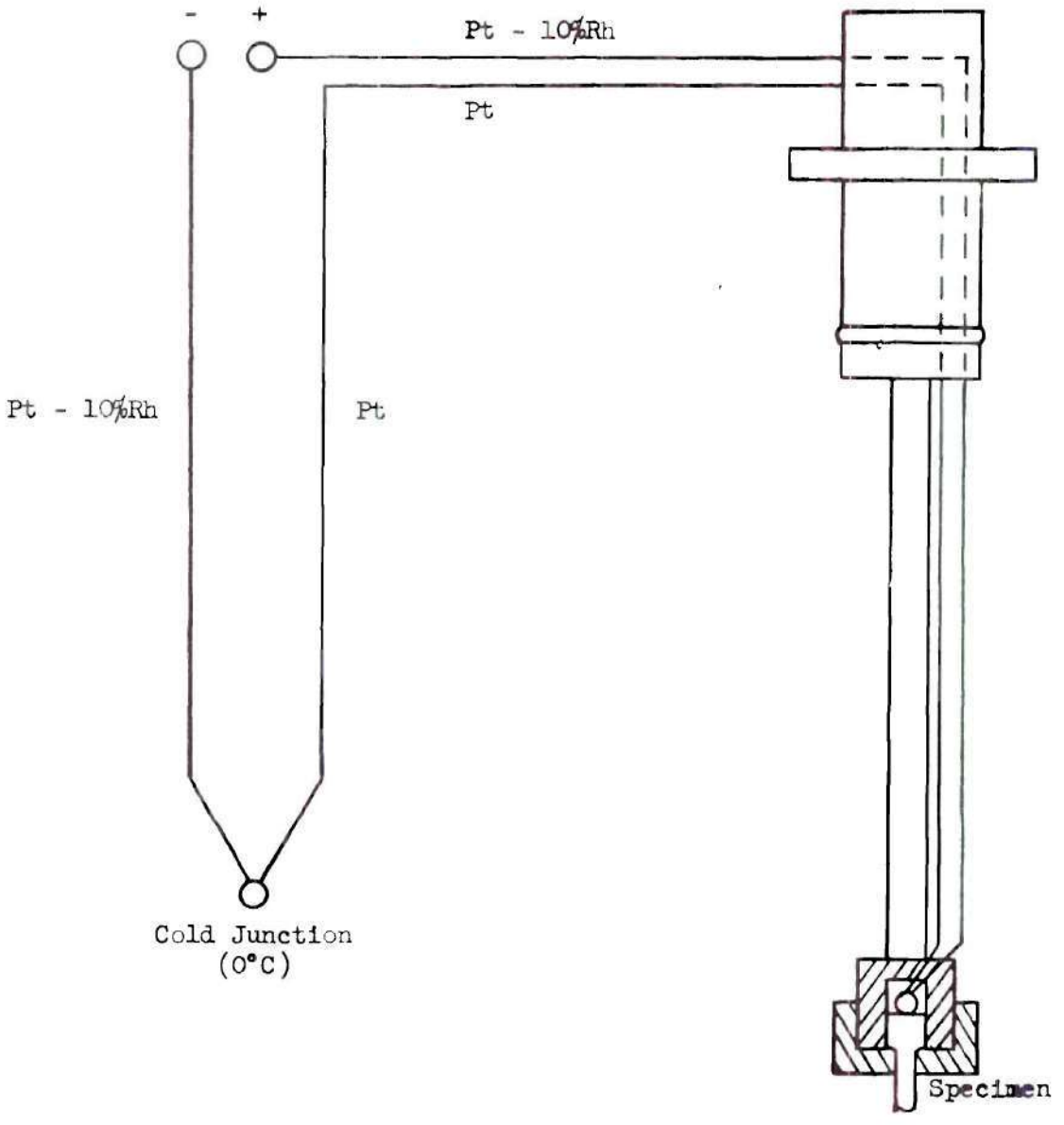

Figure 4. Schematic Diagram of Thermocouple System.

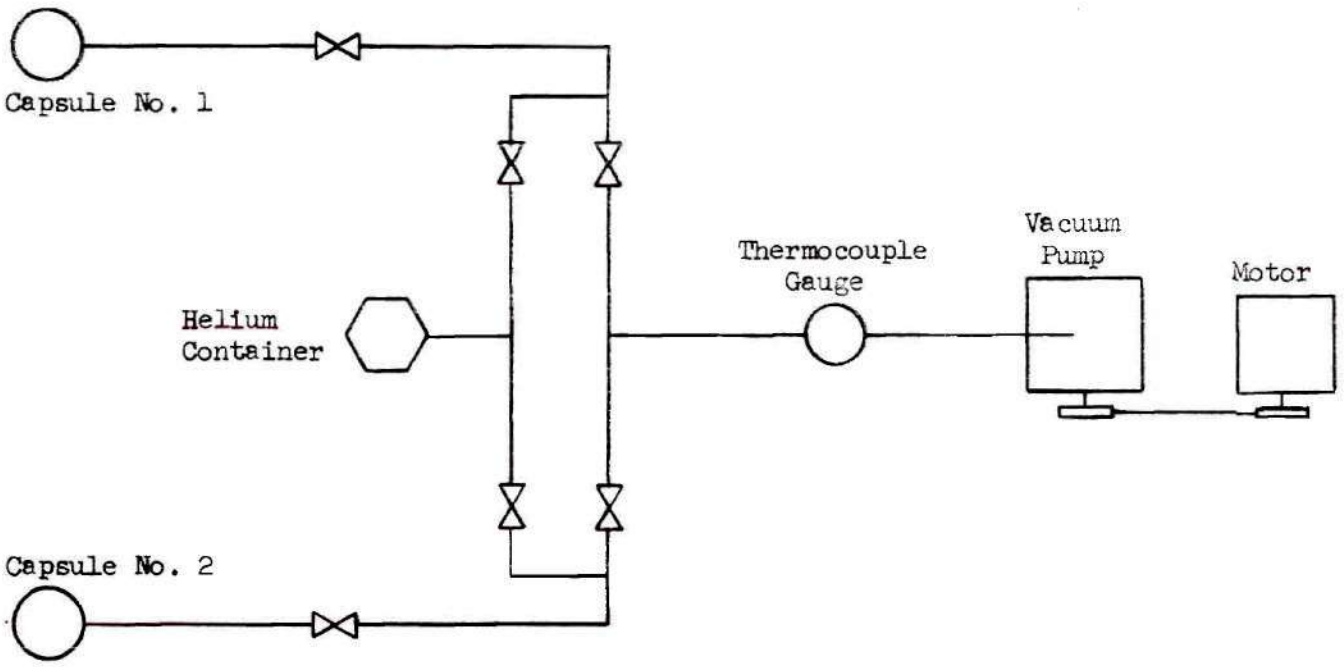

Figure 5. Schematic Diagram of Vacuum Piping Arrangement.

an inert gas.

StereoZoom Microscope with Stereo Camera

A standard Bausch and Lomb StereoZoom Microscope was used to examine the fractured specimens at magnifications of 7X to 30X. This microscope contains an adjustable power pod which makes it possible to continuously change the power to the magnification desired. A Nicholas Illuminator that can be mounted directly on the microscope or placed in any desired position on its own stand was used to light the specimen. A stereographic fixed focus 35mm camera that attaches to the microscope was used to photograph the fractured specimens.

CHAPTER III

PROCEDURE

Preparation of Specimens

The three alloys were cast in the laboratories of the Georgia Institute of Technology using Aluminum Company of America aluminum with a chemical analysis shown in Table 1 and Anaconda American Brass Company copper wire with a chemical analysis of 99.99 per cent copper with the remaining 0.01 per cent unknown.

A master ingot was cast and analyzed. The analysis by Law and Company showed that a disc from the top of the ingot contained 32.4 per cent copper and a disc from the bottom contained 32.8 per cent copper. Using this master aluminum copper alloy, alloys with nominal amounts of two, four and six per cent copper were cast. The amount of master alloy and pure aluminum used for each of the desired alloys is shown in Table 2. The chemical analysis of a disc cut from the center of each ingot is given in Table 3.

The ingots were extruded by Mr. J. A. Williams of University College, Swansea, Glamorganshire, United Kingdom. Each alloy was extruded at 400 degrees centigrade at four inches per minute into 3/8 inch diameter rods. The extruded rods were then returned to Georgia Tech where they were machined to the specimen dimensions shown in Figure 3 in the machine shop of the School of Mechanical Engineering. After machining, the specimens were stamped with identification numbers.

The first number indicated the nominal per cent copper while the following numbers indicated the specimen number for that particular alloy.

Table 1. Aluminum Chemical Analysis

Element	Per Cent	Element	Per Cent
Aluminum	99.990	Nickel	0.000
Copper	0.000	Chromium	0.000
Iron	0.001	Titanium	0.000
Silicon	0.004	Vanadium	0.000
Manganese	0.000	Boron	0.000
Magnesium	0.000	Gallium	0.003
Zinc	0.001	Zirconium	0.001

Table 2. Amount of Material Required to Make Alloys

	2.5 Pounds Alloy		2.0 Pounds Alloy	
Per Cent Copper	Pounds Master Alloy	Pounds Pure Aluminum	Pounds Master Alloy	Pounds Pure Aluminum
2	0.1533	2.3467	0.1227	1.8773
4	0.3006	2.1934	0.2454	1.7546
6	0.4599	2.0401	0.3681	1.6319

Table 3. Chemical Analysis of Alloys

Alloy Number	Per Cent Copper
2B	1.99
4B	4.02
6B	6.11

Experimental Procedure

The test specimens used were approximately one and one-eighth inches long with a cross sectional area of 0.02 square inches. These specimens were placed in the vacuum capsules, and the capsules were evacuated. While this was being done the furnaces were turned on and allowed to heat up. When the furnaces had reached the vicinity of the test temperature, the capsules containing the test specimens were placed in them. The temperature of the specimen was checked periodically to insure that it did not overshoot too much. If this happened the specimen was cooled down 50 to 75 degrees centigrade and then reheated. When the temperature of the specimen approached the desired test temperature, the pull assembly was connected to the Instron machine. Then when the temperature remained stable for two to three minutes, the test was initiated by starting the chart recorder and the crosshead drive simultaneously. During the test the potentiometer was checked to obtain the exact test temperature and the vacuum gauge checked to assure that the vacuum system was working satisfactorily.

The chart was observed to determine when fracture of the specimen occurred. Immediately after this the Instron machine was stopped and the vacuum capsule removed from the furnace and placed on a stand. The valve to the vacuum pump was closed and another valve opened to allow inert gas to enter the vacuum capsule. In this manner the fractured specimen was cooled rapidly in an inert atmosphere to prevent oxidation. The cooling rate was then checked over a period of three minutes using the thermocouple and potentiometer. The test rate, test temperature, chart speed, vacuum and cooling rate were all recorded

on a data sheet. When the specimen had cooled down to 200 degrees centigrade it was taken out of the vacuum capsule and exposed to the atmosphere. However, very little oxidation occurred at or below this temperature.

While the maximum load of the load cell used was 1000 pounds, the sensitivity scale was adjusted for most runs to where full scale deflection was 100 pounds. At lower temperatures the scale was usually set for 200 pounds full scale deflection even though higher scales were necessary for some tests.

Because the response time of the chart recorder limits the crosshead speed to one inch per minute for use with the recorder, it was necessary to use an oscilloscope with a polaroid camera attachment to record the data for the 20.0 inches per minute strain rate. The oscilloscope was connected to the output of the recorder amplifier through another external amplifier.

The test procedure was the same as described above except that the camera shutter was opened as the test was started and held open until after fracture had occurred. The necessary data was recorded and the photograph developed. This photograph served as the load versus time curve that was normally obtained on the chart recorder.

Microscopic Examination

The fractured specimens were examined under a microscope at magnifications of 7X to 30X. Comments were recorded, and photographs of typical results as well as of unusual occurrences were made using a camera attachment available with the microscope.

Accuracy of Measurements

The experimental results were obtained from the load verus time curves obtained from the Instron Tensile Testing Instrument for each specimen. These results are tabulated in Appendix A along with an explanation of each type of calculation.

The measured load was determined to be plus or minus one half pound of the actual applied load because of a tendency of the O-rings in the vacuum capsule to grab the sides of the capsule. The resulting error could have caused the stress calculations to be 25 to 50 pounds per square inch from the actual value.

The strain, or percentage elongation, was also measured from the load versus time graph. The elongations determined from the graph usually agreed within two per cent with the elongation obtained from actual specimen measurement for the ductile fractures. For brittle fractures actual specimen measurement was impossible because of the movement of individual grains.

The accuracy of the time measurements varied according to the chart speed. For the slower speed of one half inch per minute, the accuracy was within plus or minus ten per cent; for 50 inches per minute, it was plus or minus two tenths of one per cent. The accuracy was generally within plus or minus two per cent.

The per cent rough fracture area was estimated after examination of the fractured surfaces at magnifications of about 30X.

CHAPTER IV

DISCUSSION OF RESULTS

General Graphs of Stress to Fracture Versus Temperature

Graphs of stress to fracture versus temperature for the three aluminum-copper alloys tested are presented in Figures 6 through 15. These graphs have the same general characteristics as those determined by other investigators for similar alloys. The stress to fracture decreases rapidly between 200 and 300 degrees centigrade for all three alloys tested. Above this temperature range the stress to fracture continues to decrease, but for a given temperature increment there is a decrease in the stress increment as the temperature increases. As the solidus temperature is passed the stress to fracture drops to very low values with only a small increase in temperature. Once it has dropped to very low values in the temperature range above the solidus, the stress to fracture decreases gradually to zero as the grain boundaries become completely covered with liquid. The temperature at which the stress to fracture drops to zero in each alloy is determined to a large extent by the distribution of the liquid phase which is controlled by the dihedral angle of the alloy.

From the graphs shown in Figures 6 through 15 it can be seen that increasing the copper content increases the stress to fracture for the alloy in the region below the solidus. The strain rate also has an effect on the stress to fracture, and this will be discussed in the next section.

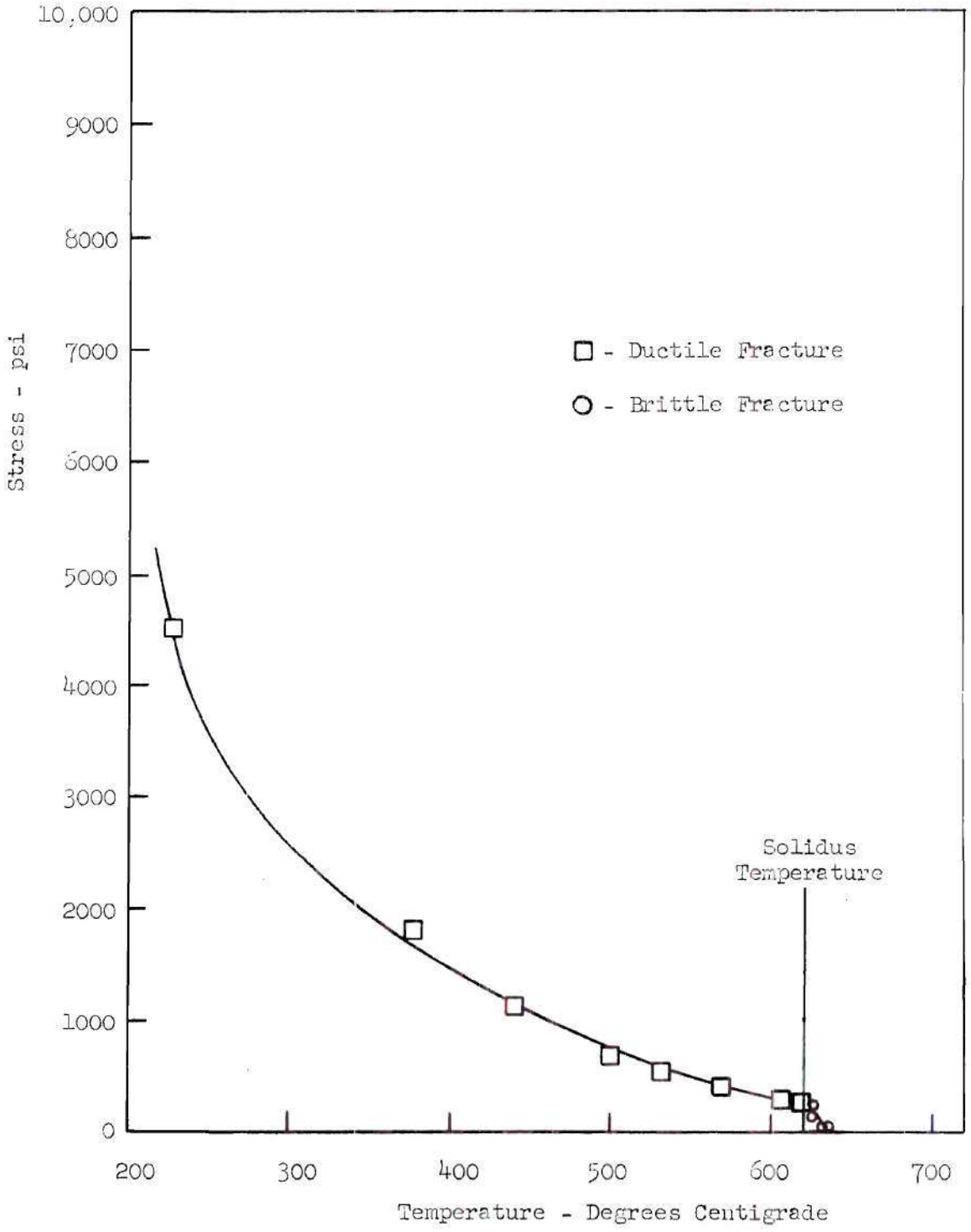

Figure 6. Stress to Fracture Versus Temperature for Two Per Cent Copper-Aluminum Alloy Tested at a Strain Rate of 0.02 Inches Per Minute.

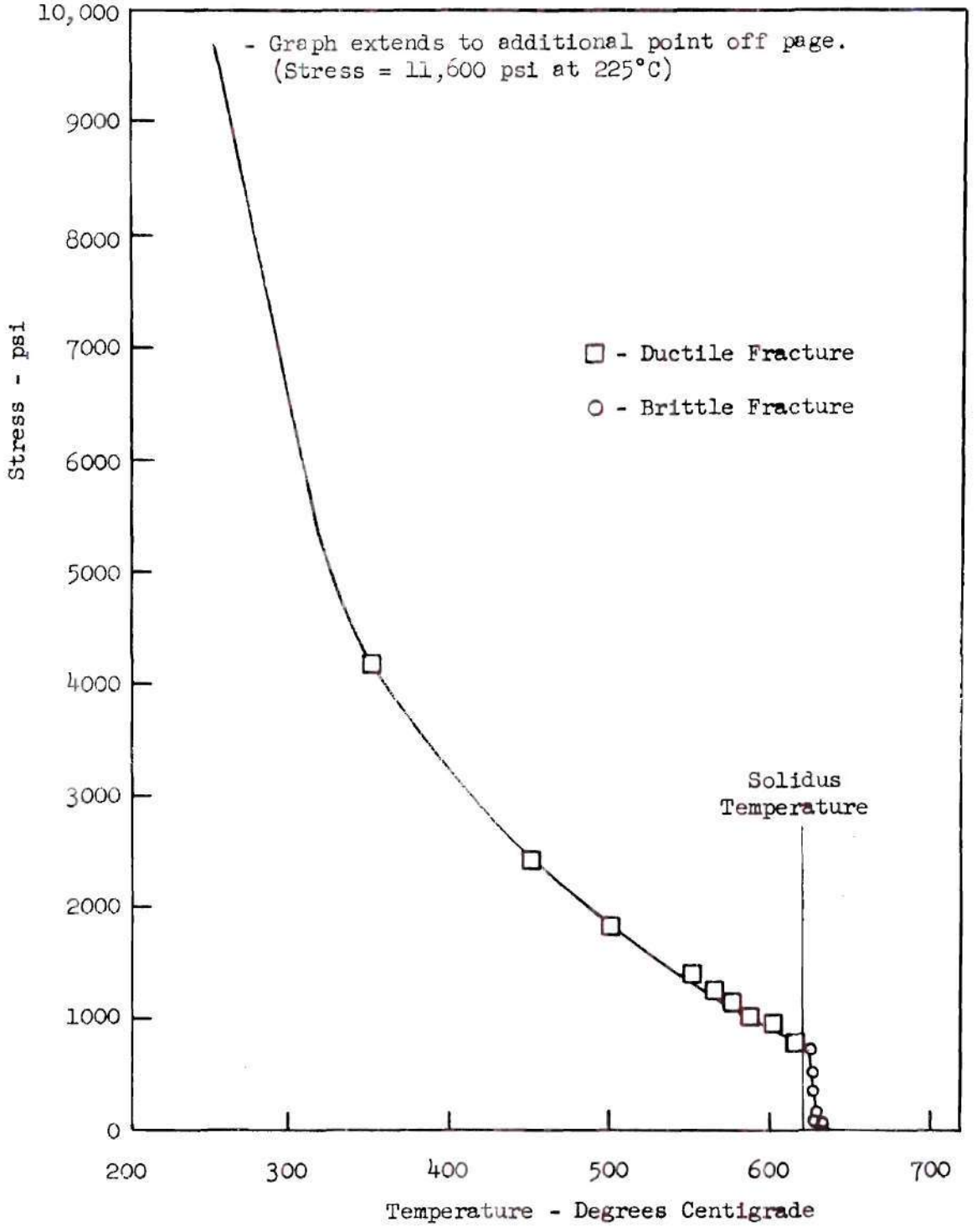

Figure 7. Stress to Fracture Versus Temperature for Two Per Cent Copper-Aluminum Alloy Tested at a Strain Rate of 1.0 Inches Per Minute.

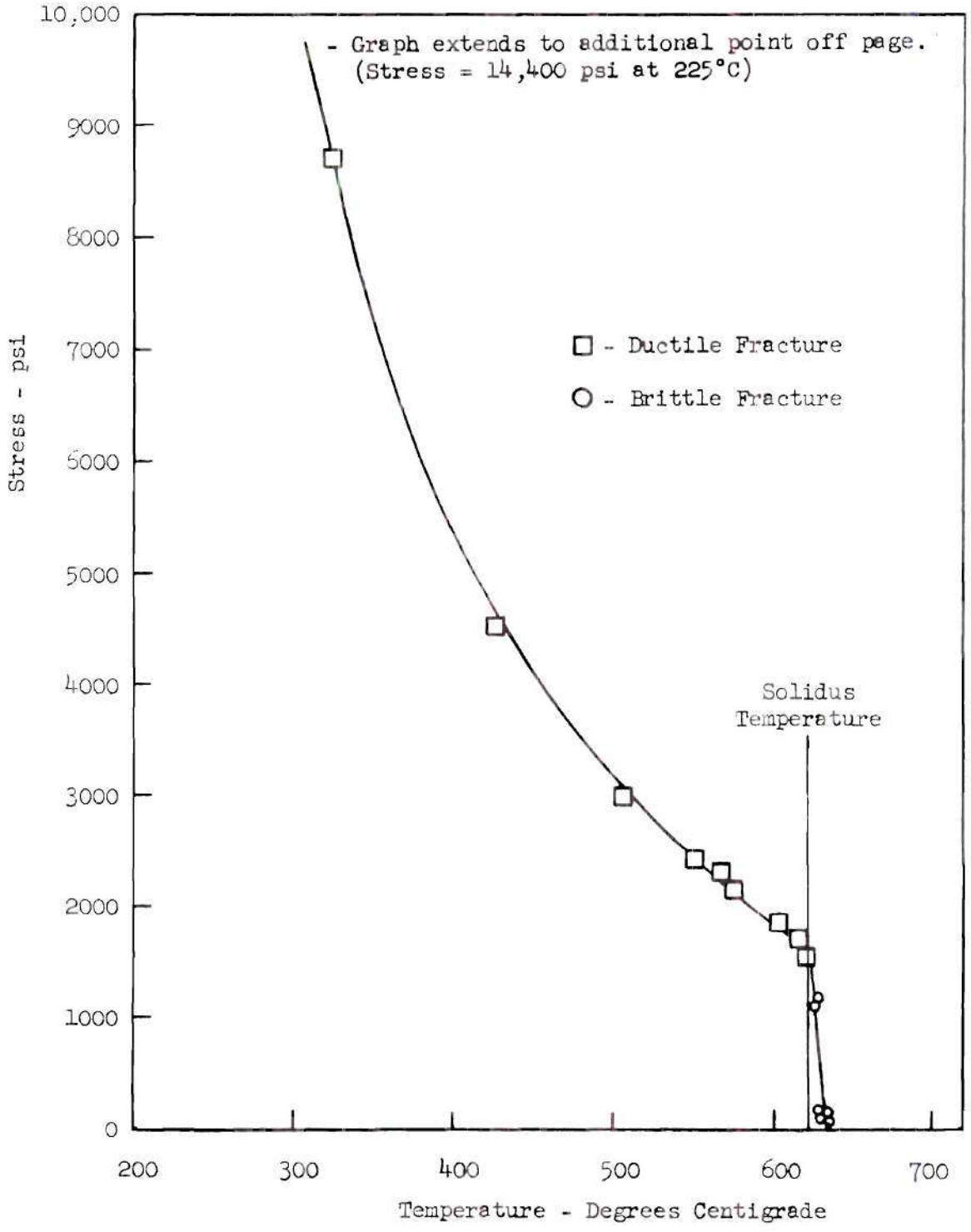

Figure 8. Stress to Fracture Versus Temperature for Two Per Cent Copper-Aluminum Alloy Tested at a Strain Rate of 20.0 Inches Per Minute.

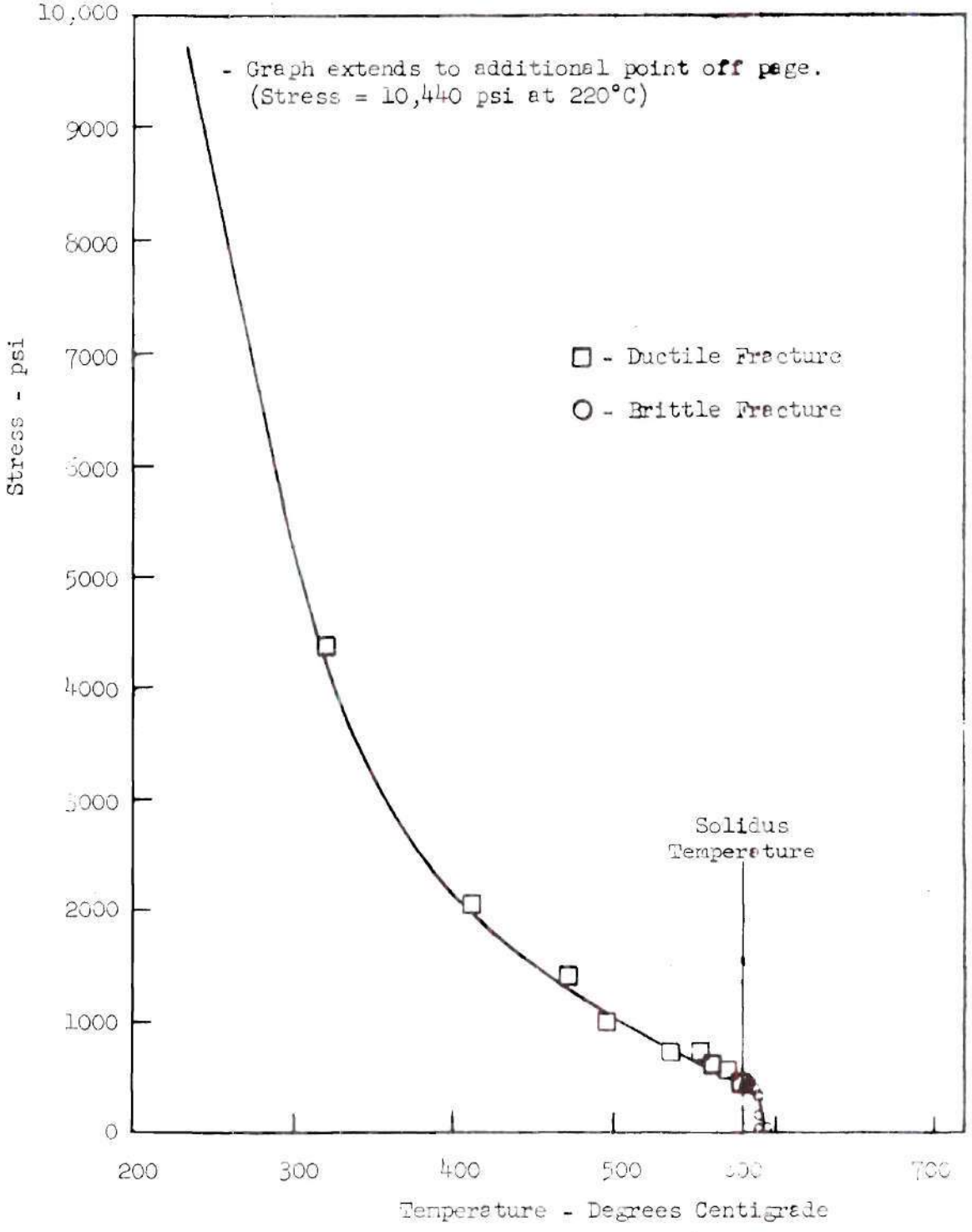

Figure 9. Stress to Fracture Versus Temperature for Four Per Cent Copper-Aluminum Alloy Tested at a Strain Rate of 0.02 Inches Per Minute.

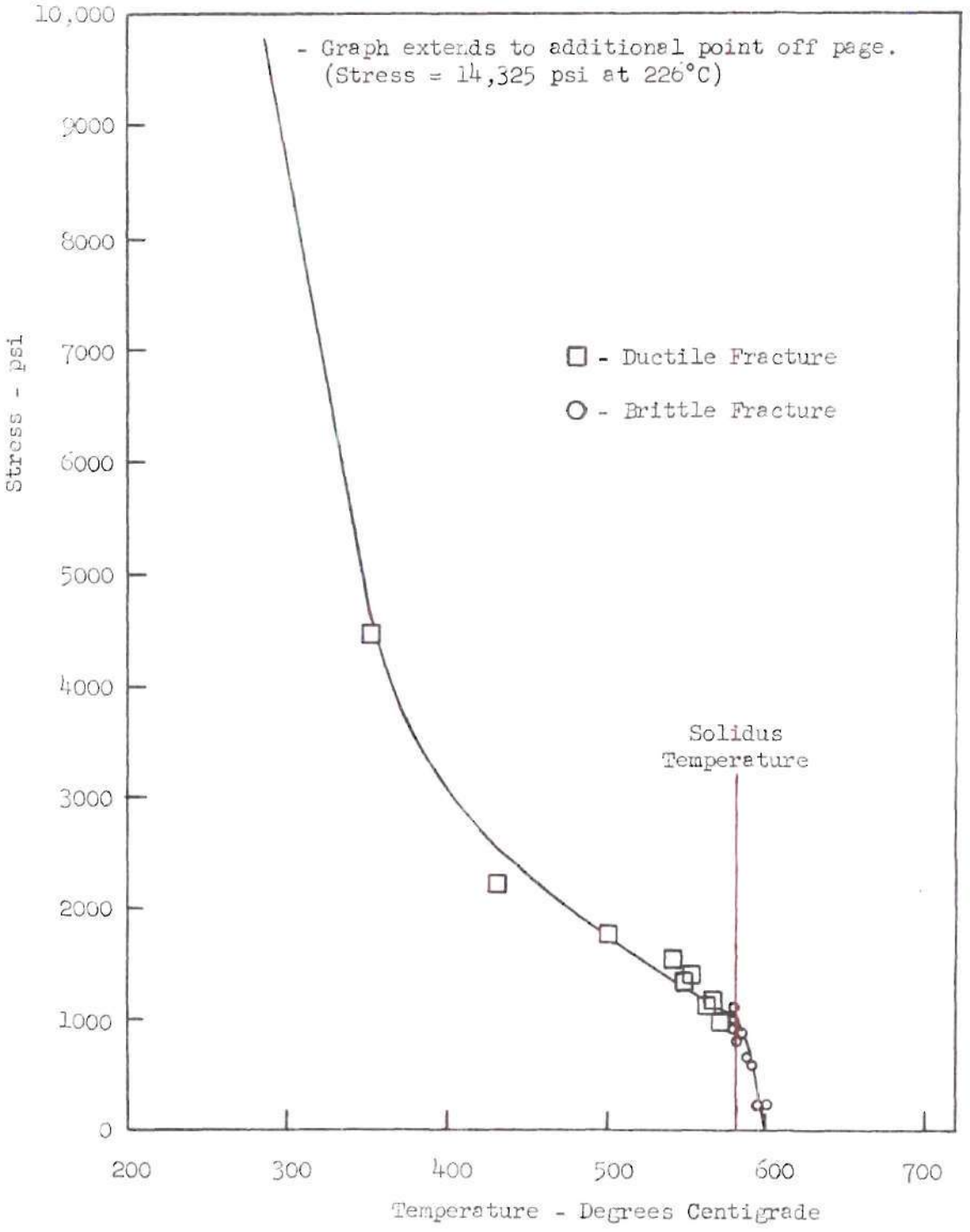

Figure 10. Stress to Fracture Versus Temperature for Four Per Cent Copper-Aluminum Alloy Tested at a Strain Rate of 0.20 Inches Per Minute.

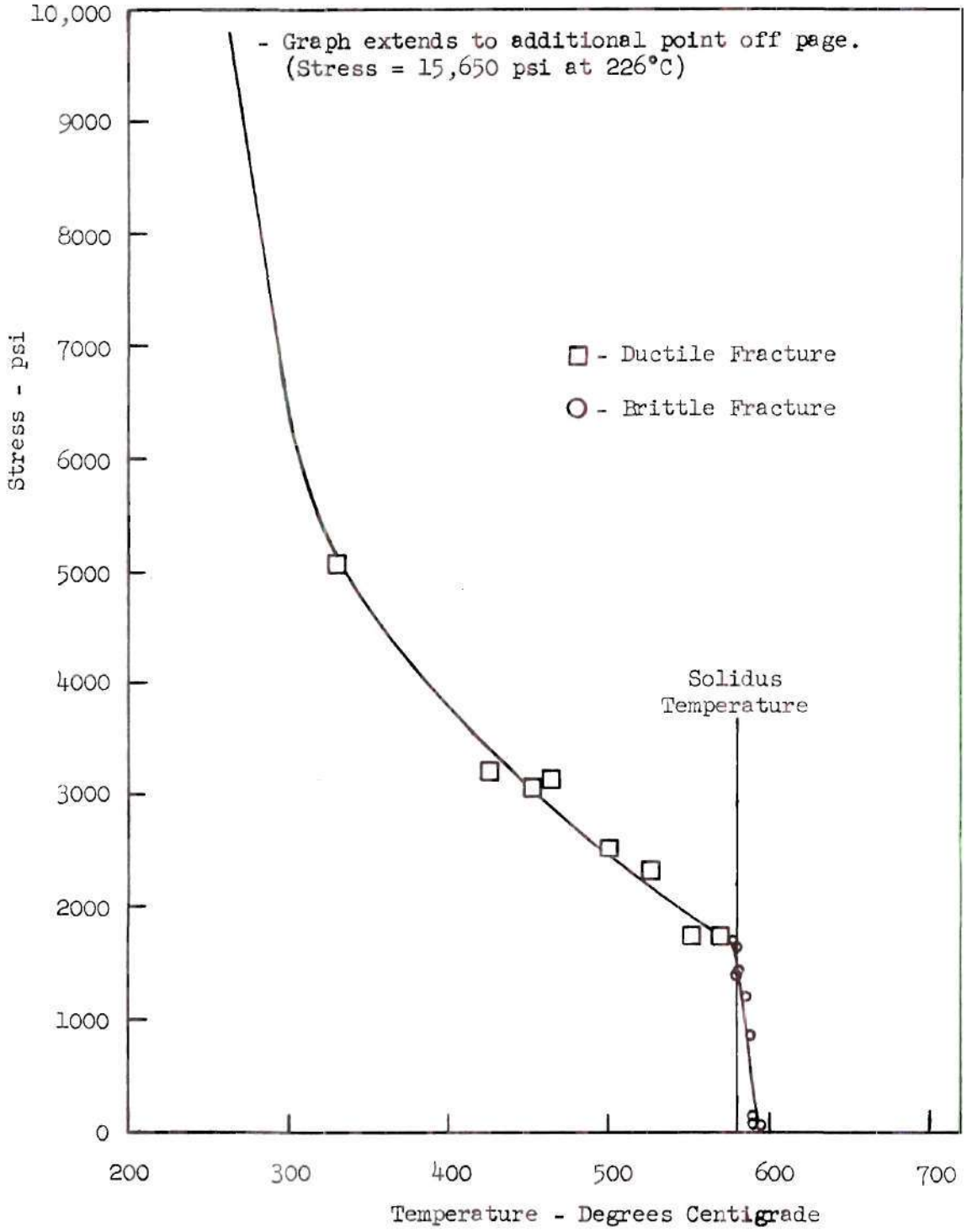

Figure 11. Stress to Fracture Versus Temperature for Four Per Cent Copper-Aluminum Alloy Tested at a Strain Rate of 1.0 Inches Per Minute.

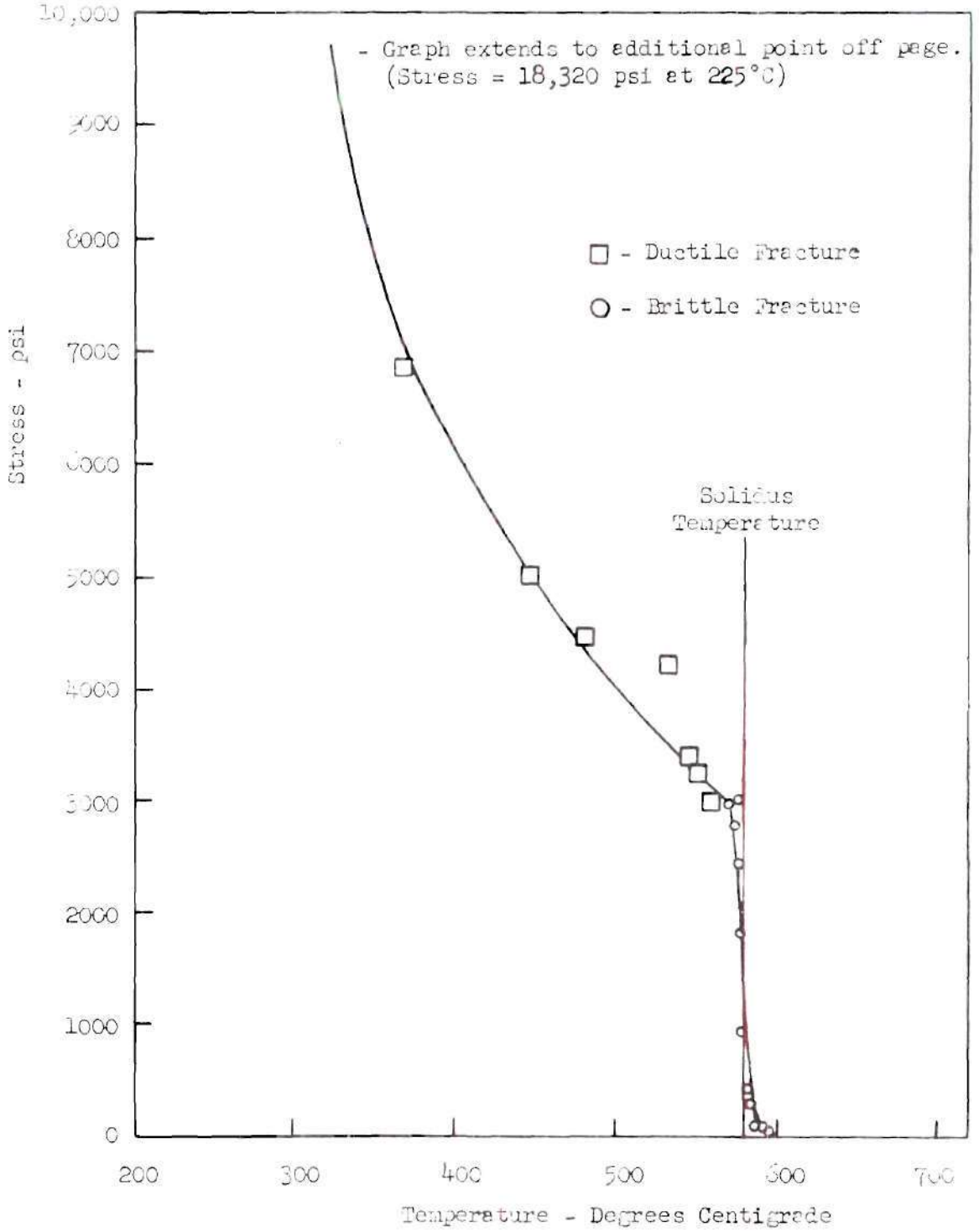

Figure 12. Stress to Fracture Versus Temperature for Four Per Cent Copper-Aluminum Alloy Tested at a Strain Rate of 20.0 Inches Per Minute.

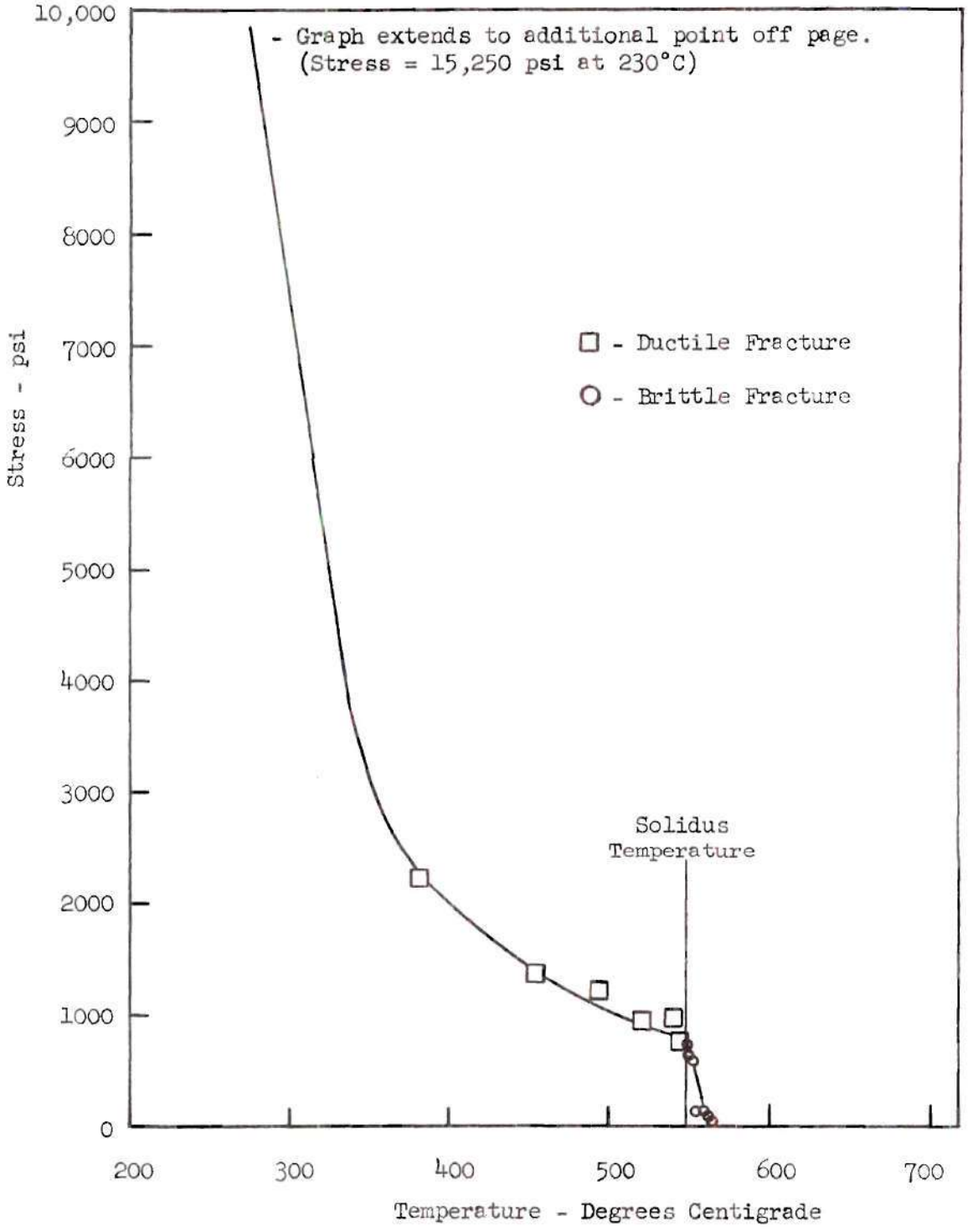

Figure 13. Stress to Fracture Versus Temperature for Six Per Cent Copper-Aluminum Alloy Tested at a Strain Rate of 0.02 Inches Per Minute.

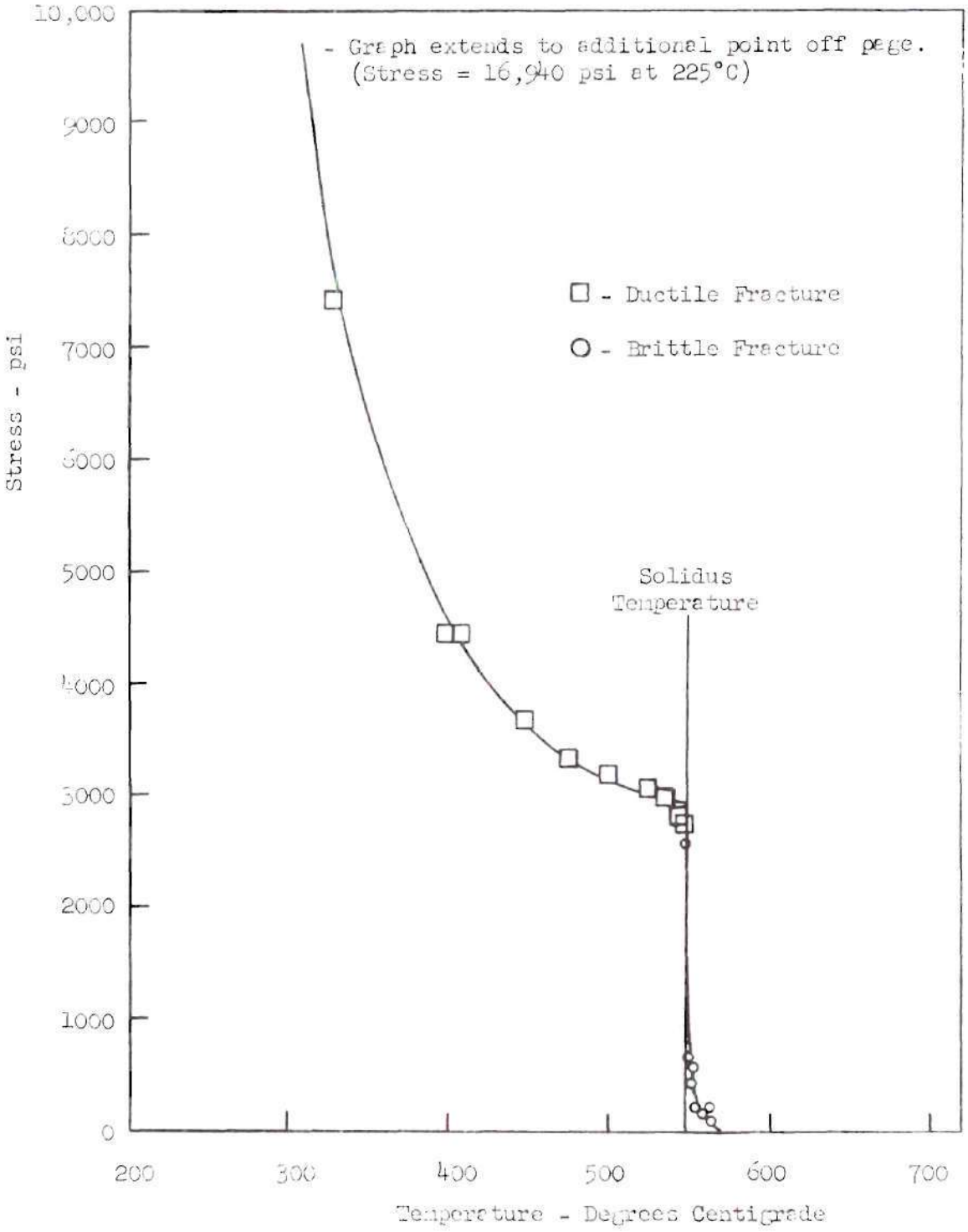

Figure 14. Stress to Fracture Versus Temperature for Six Per Cent Copper-Aluminum Alloy Tested at a Strain Rate of 1.0 Inches Per Minute.

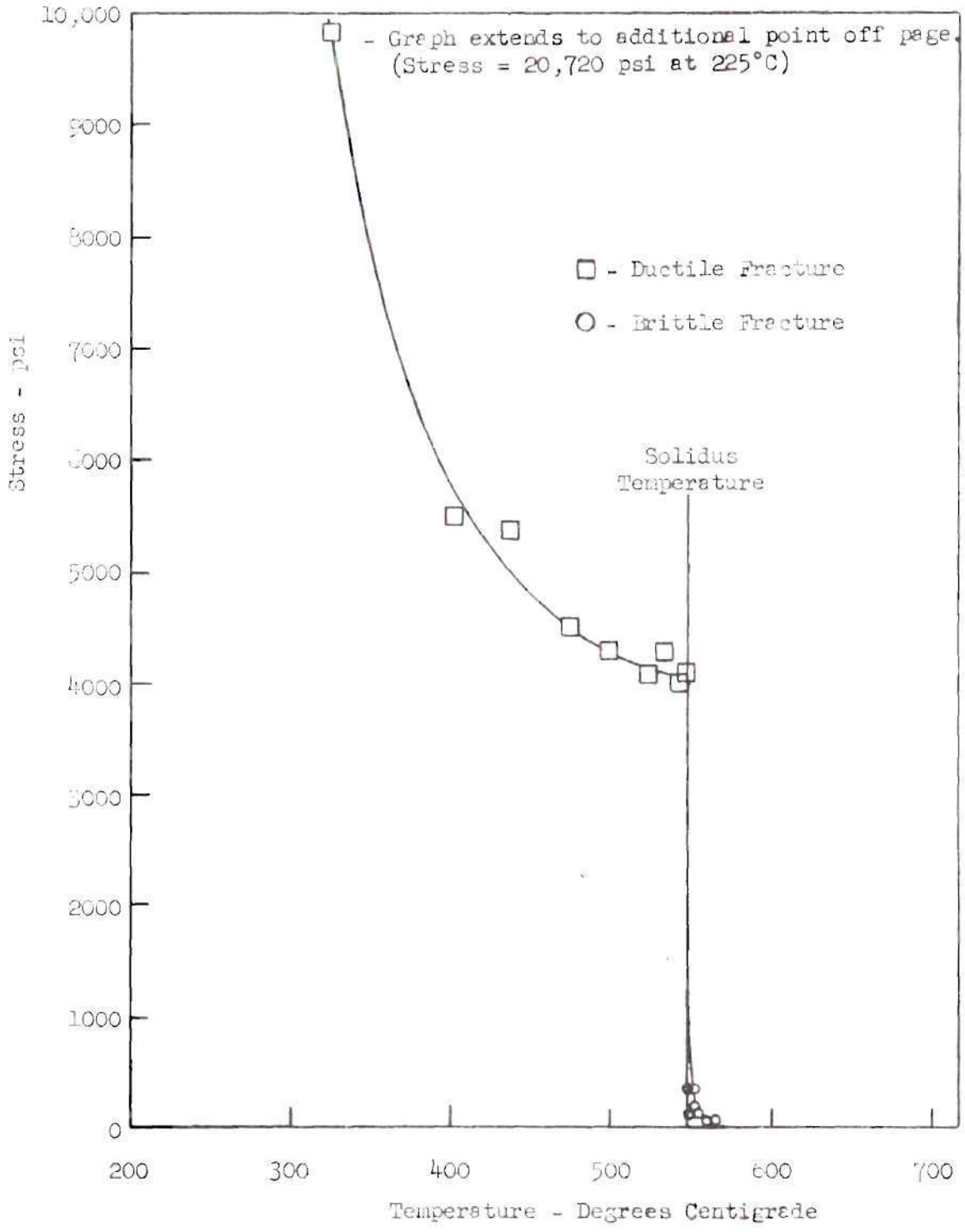

Figure 15. Stress to Fracture Versus Temperature for Six Per Cent Copper-Aluminum Alloy Tested at a Strain Rate of 20.0 Inches Per Minute.

Effect of Strain Rate on Stress to Fracture Versus Temperature Graphs

Figures 16 through 20 are presented to show more clearly the effect of varying the strain rate on the stress to fracture versus temperature graphs in the region of the solidus. These graphs show several important results. (1) An increase in the strain rate increases the stress to fracture in the region below the solidus. (2) An increase in the strain rate has only a small effect on the slope of the stress to fracture curve in the region just below the solidus temperature. (3) In the region just above the solidus temperature, an increase in the strain rate has a marked effect on the slope of the stress to fracture versus temperature curve. The slope of the curve in this region increases quickly when the strain rate is increased. This change in slope indicates that the strength of the alloy decreases faster per fixed temperature increment for the higher strain rates than for the lower strain rates. (4) However, as the temperature increases further above the solidus temperature, the stress to fracture appears to be independent of the strain rate. The alloys lose their coherency about the same temperature regardless of the strain rate. In this region the amount of the grain boundaries that are covered with liquid is dependent on the dihedral angle of the alloy. It appears that for this reason the strength at temperatures 10 to 15 degrees centigrade above the solidus is dependent on the dihedral angle, which approaches zero in this temperature range, thus allowing the grain surfaces to become covered with liquid; and therefore the strain rate has only a small effect on the strength.

Another very important result can be seen in the lower portion of Figure 17. For the strain rate of 20.0 inches per minute the strength

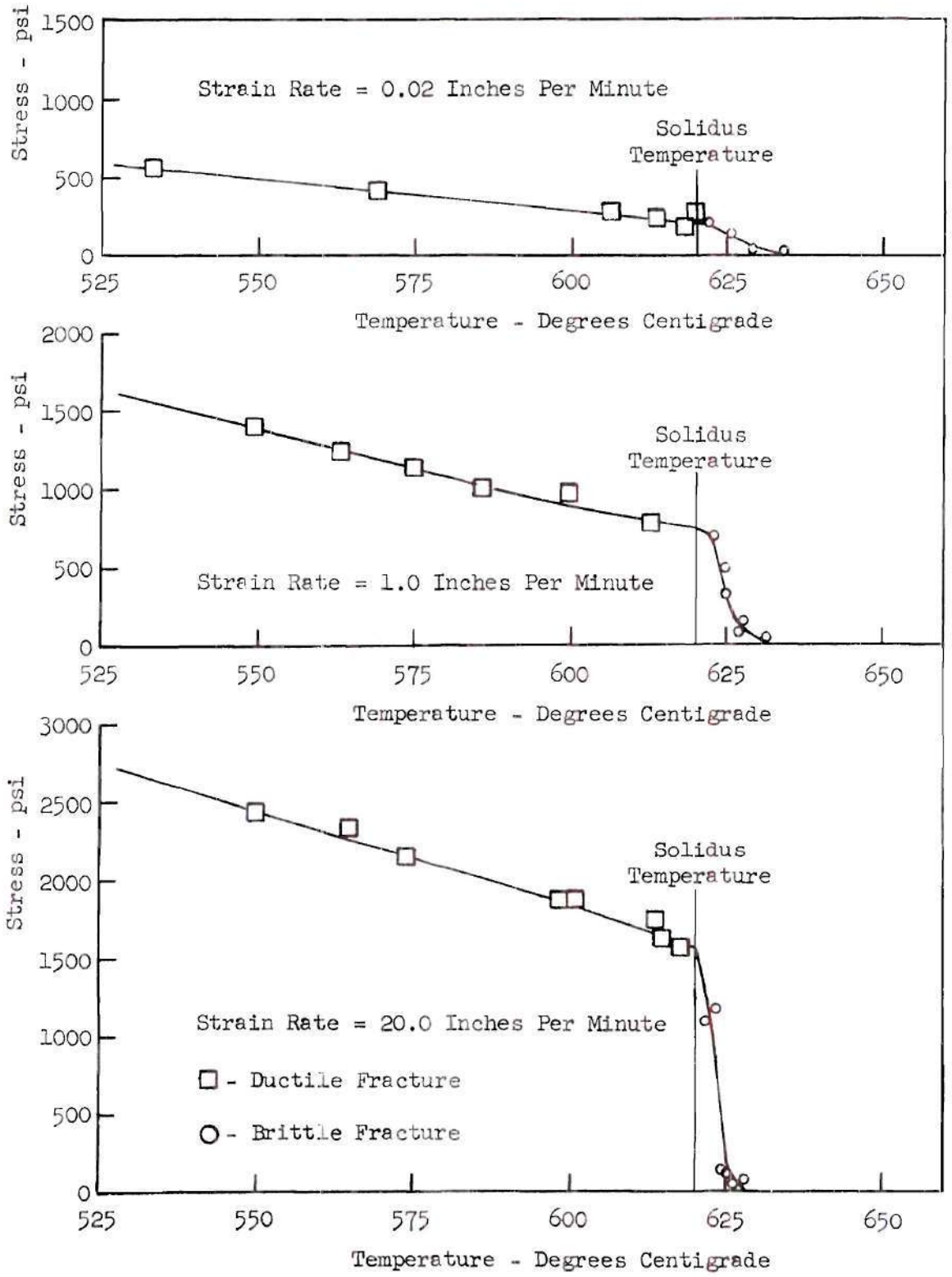

Figure 16. Stress to Fracture Versus Temperature for Two Per Cent Copper-Aluminum Alloy.

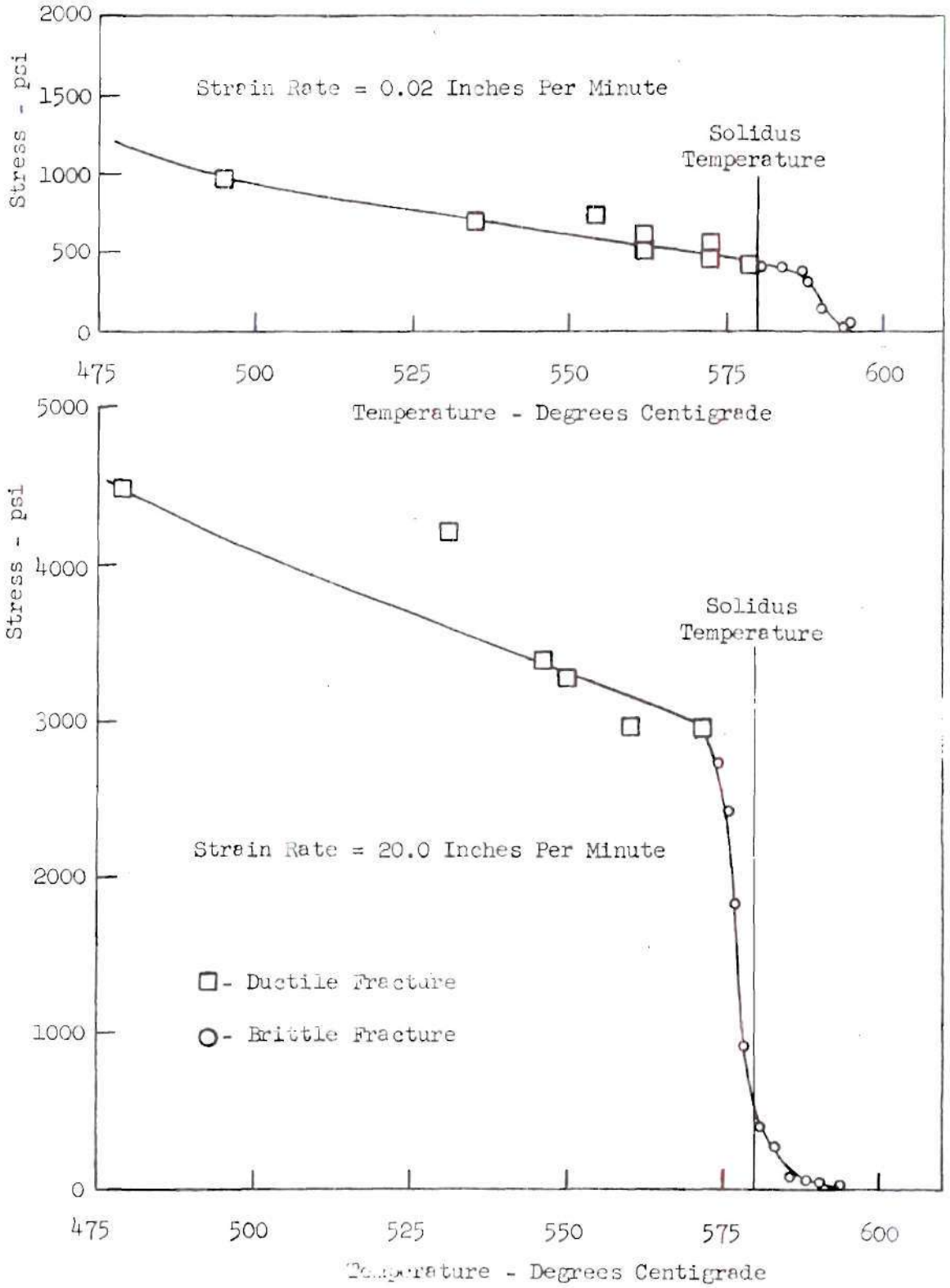

Figure 17. Stress to Fracture Versus Temperature for Four Per Cent Copper-Aluminum Alloy.

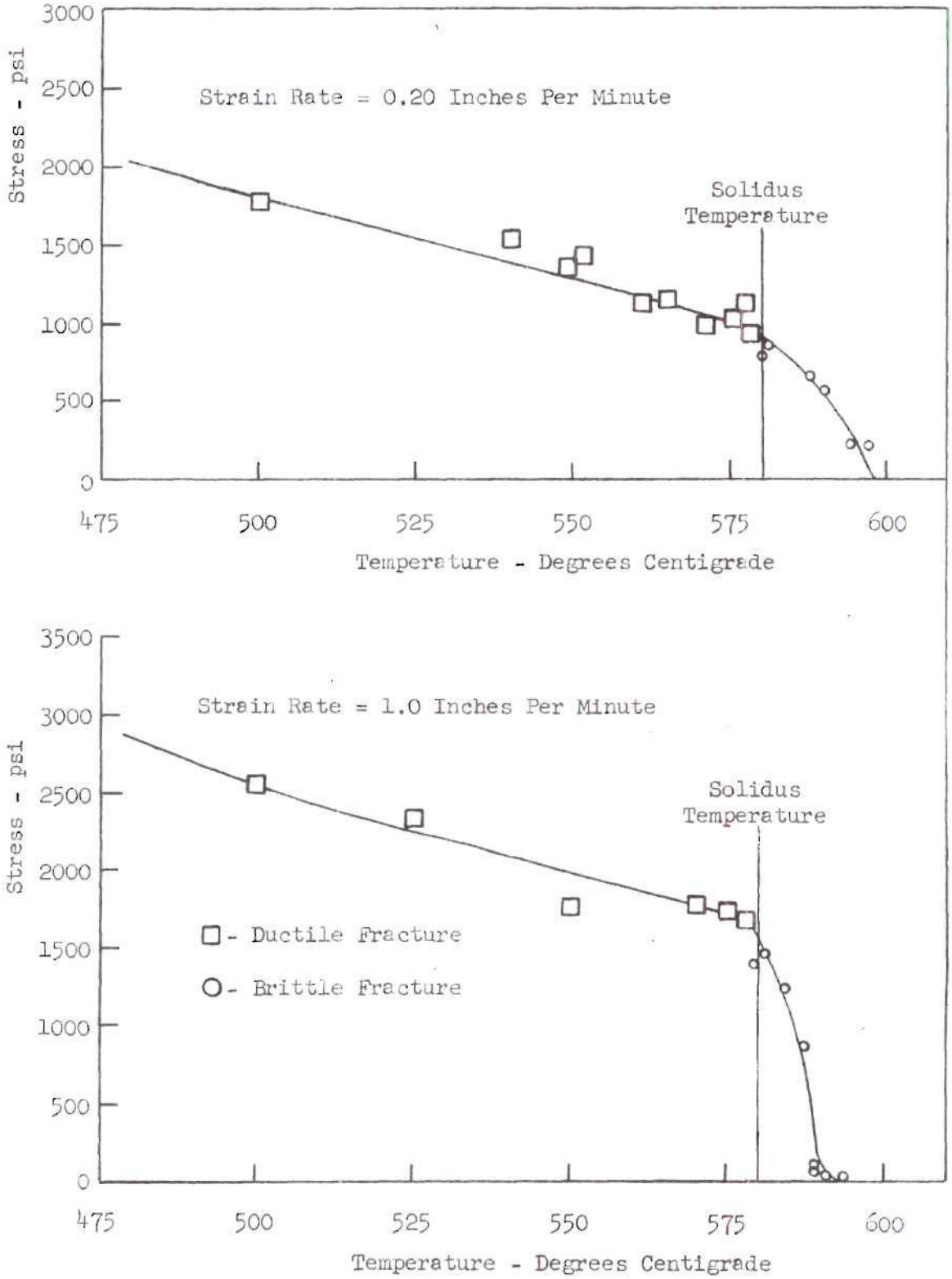

Figure 18. Stress to Fracture Versus Temperature for Four Per Cent Copper-Aluminum Alloy.

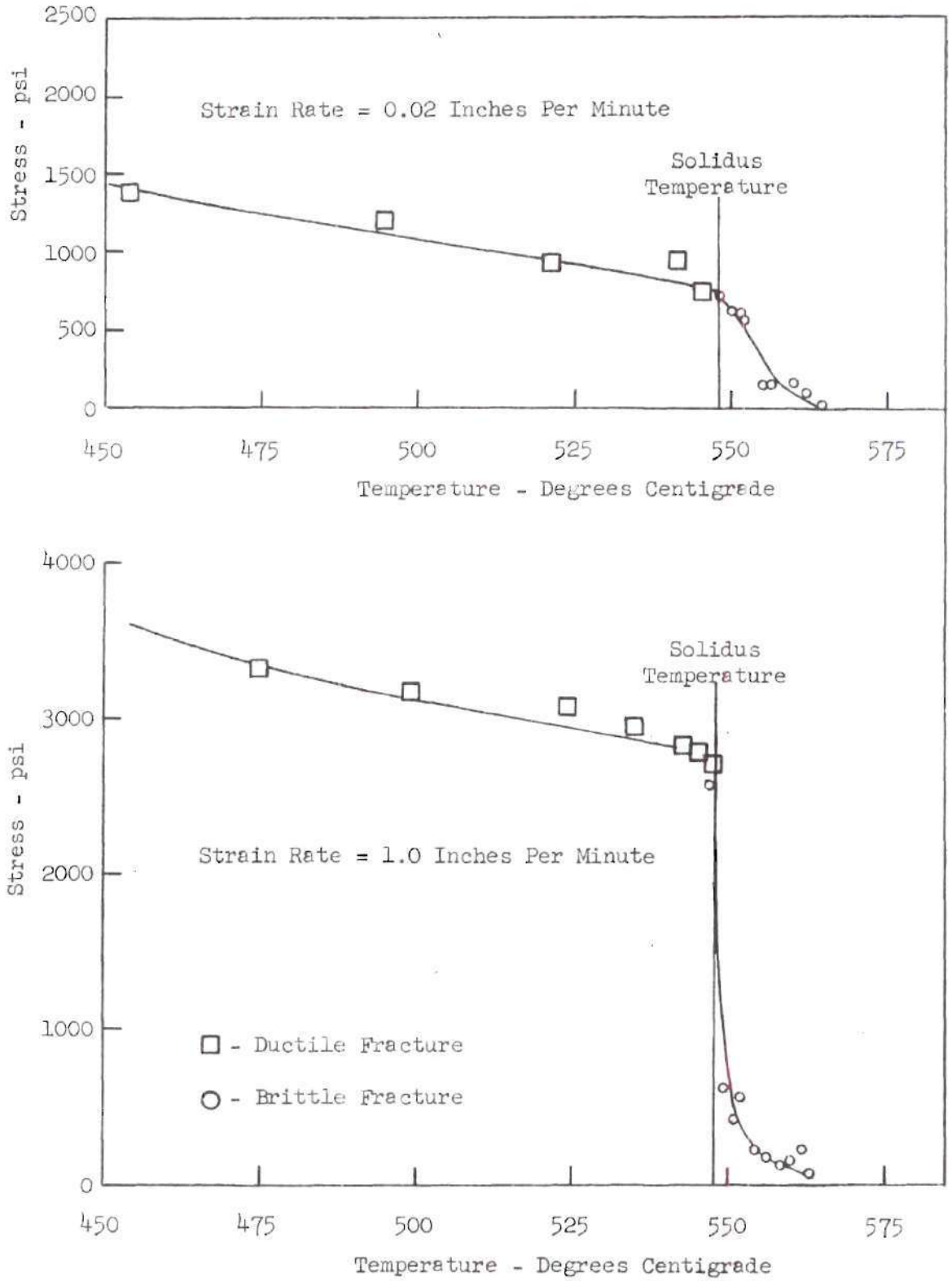

Figure 19. Stress to Fracture Versus Temperature for Six Per Cent Copper-Aluminum Alloy.

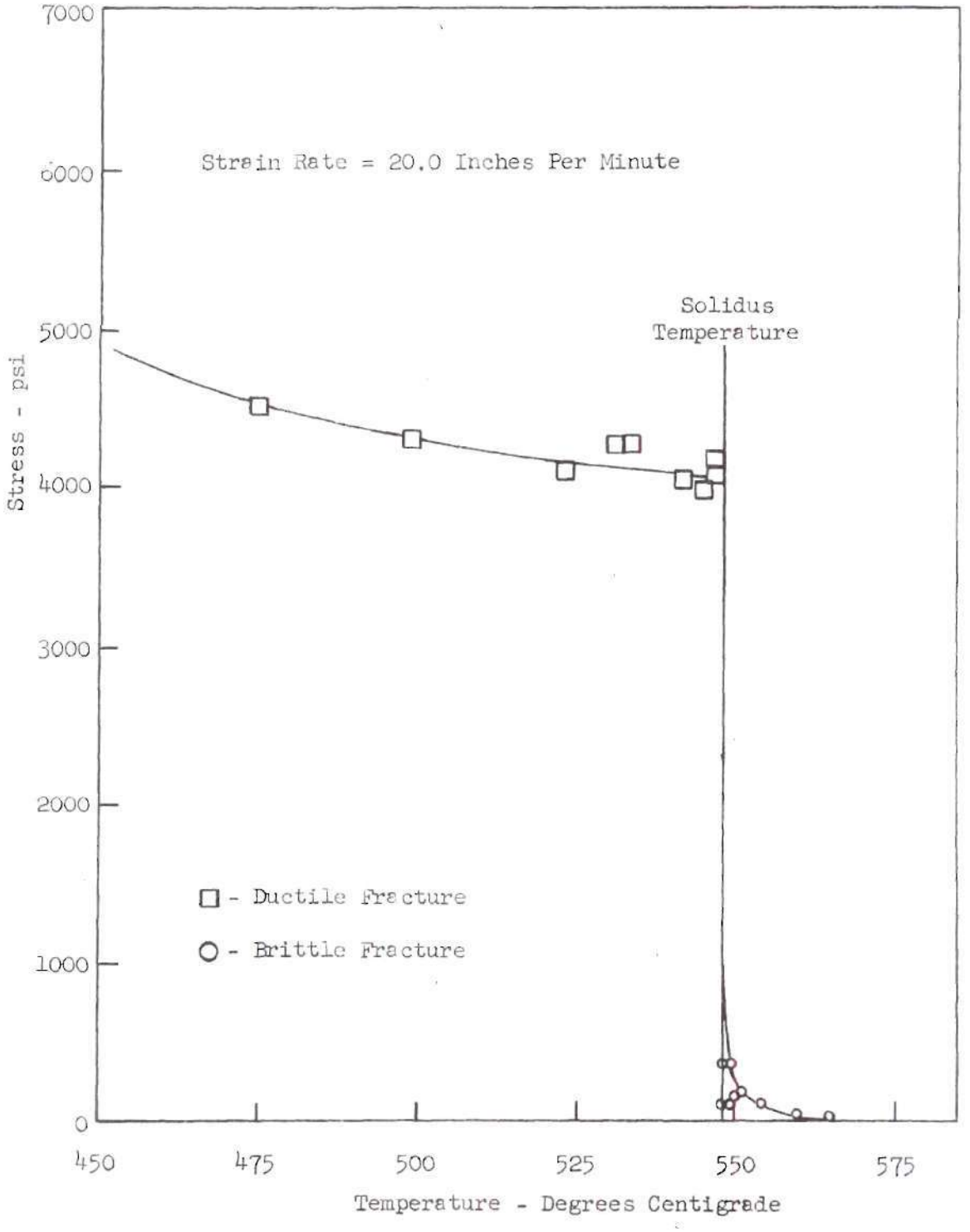

Figure 20. Stress to Fracture Versus Temperature for Six Per Cent Copper-Aluminum Alloy.

of the four per cent copper-aluminum alloy falls off quickly before the solidus temperature is reached. This decrease in strength is probably caused by the higher energy input per unit of time for the higher strain rates. During deformation the energy is converted into heat which raises the temperature of the grain boundaries enough to cause localized melting in the fracture zone of the four per cent alloy. Then brittle fracture occurs and the strength of the alloy decreases quickly, giving the appearance that the solidus temperature has been reached.

Of the total volume, 0.02 square inches cross-sectional area by 1.125 inches long for a typical specimen, of a specimen the portion in which brittle fracture occurs is estimated to be about five per cent. This estimate is based on the fact that the length of the specimen in which the brittle fracture took place (the fracture zone) was usually about one sixteenth of an inch, or about five per cent of the length of the specimen. Calculations, Appendix C, show that to increase the temperature of five per cent of the total volume one degree centigrade requires about 0.403 inch-pounds if the heat transfer out of this volume is neglected. At temperatures near the solidus the energy put into a specimen between maximum load and failure is believed to go into the fracture region. For the four per cent specimen tested at a strain rate of 20.0 inches per minute at 578 degrees centigrade the amount of energy put into the fracture region was about one inch-pound in one-fifth second, which is equivalent to five inch-pounds per second. The amount of energy put into the fracture region of the four per cent specimen tested at a strain rate of 1.0 inches per minute at 578 degrees centigrade was about 0.240 inch-pounds in six seconds, or 0.040 inch-pounds per second. For

the 0.20 inches per minute strain rate the amount of energy was about 0.100 inch-pounds in nine seconds, or 0.011 inch-pounds per second. Therefore it can be seen that it is possible to raise the temperature of the specimen several degrees if the energy input is high and the time interval for the energy input is short, as in the case for the strain rate of 20.0 inches per minute.

This melting of grain boundaries at high strain rates does not appear to occur in either the two per cent or six per cent alloys. The two per cent alloy is not as strong as the other two alloys; consequently not as much energy is converted to heat while the material is deforming plastically. The energy converted to heat in the fracture zone for the two per cent alloy specimens at temperatures near the solidus was about 1.25 inch-pounds per second, and for the four per cent alloy specimens it was about five inch-pounds per second. As the larger grained two per cent alloy is deformed plastically there is not enough heat generated to melt the grain boundaries and cause brittle fracture below the solidus since the energy input per unit time is small.

For the six per cent alloy it is believed that the smaller grain size (grain size numbers three to two) is the reason why brittle fracture does not occur at temperatures just below the solidus when the high strain rates are used. For a given per cent liquid, the film thickness is going to decrease as the grain size decreases because the ratio of surface area to volume varies with the grain diameter and is greater for the smaller grains than for the larger grains. The heat generated melts a given volume of the alloy, but the resulting liquid is not enough to cover the grain surfaces and permit a brittle class of fracture. There-

fore the specimen continues to deform plastically with the corresponding elongation until the strength decreases to a point where fracture occurs.

Another point of interest is the large drop in stress to fracture with a small increase in temperature shown in the bottom curve of Figure 19 and in Figure 20 for the six per cent alloy. The reason for this rapid drop in stress is that once the solidus temperature of the six per cent alloy is reached, 1.5 per cent of the metal melts before the temperature increases further. The grain boundaries become mostly covered with liquid, and the result is brittle fracture with low strength.

The large drop in stress to fracture with a small increase in temperature in the range above the solidus does not appear to occur for the six per cent alloy when tested at the strain rate of 0.02 inches per minute, as is shown in the upper curve in Figure 19. It was stated by Eborall and Gregory[4] that the stress required to cause fracture is decreased when the micro-cracks present are filled with liquid. It is proposed that for the slow strain rates metal at the fracture surface is not melted as in the case for high strain rates.

Since the new fracture surface is not covered by a thin liquid layer resulting from the localized heating due to the plastic deformation, the liquid metal flows into the crack more slowly because of the surface tension forces between the liquid and the solid, compared to the lack of surface tension between two liquid interfaces.

It was also observed that increasing the strain rate increased the strength of the alloy when tested at temperatures around 225 degrees centigrade. This increase in strength for each alloy is shown in Table 4. Although only three different strain rates were used, the

data presented in Table 4 shows a general trend of increasing stress to fracture with an increase in strain rate. It should also be noted that the grain sizes in the two per cent alloy were about four times as large as the grain sizes in the six per cent alloy and about one and one half times as great as the grain sizes in the four per cent alloy.

Table 4. Values of Stress to Fracture for Specimens Tested in the Vicinity of 225°C

Two Per Cent Alloy			Four Per Cent Alloy			Six Per Cent Alloy		
Strain Rate in/min	Temp °C	Stress psi	Strain Rate in/min	Temp °C	Stress psi	Strain Rate in/min	Temp °C	Stress psi
0.02	230	4500	0.02	220	10440	0.02	230	15250
1.0	225	11600	1.0	226	15650	1.0	225	16940
20.0	225	14400	20.0	225	18320	20.0	225	20720

Types of Fracture

In this investigation the aluminum-copper specimens were tested from 225 degrees centigrade up to and including the solidus temperature for all three alloys. From an examination of these specimens under a microscope it was determined that there were two types of fracture present. Investigations at temperatures above the solidus have shown that a third type of fracture exists in that region.[12] The first type of fracture occurs well below the solidus while the second type occurs in the region of the solidus. The type of fracture is independent of the alloy content, but dependent mainly on the relation of the temperature of the specimen to the solidus temperature of the alloy. Also there is

some dependence on the strain rate, which was discussed in the previous section. There is no sharp transition from one type of fracture to another, but instead a gradual one as the temperature of the specimen is increased. A discussion of each type of fracture follows.

Fracture Below the Solidus

For all three alloys the failure at temperatures well below the solidus was a ductile type which resulted in the typical cup-and-cone fracture. Figures 21 through 24 show that the ductility increases as the temperature increases until about 20 to 50 (usually about 50) degrees centigrade below the solidus. Then the ductility decreases until it reaches very small values at the solidus temperature. This ductility will be discussed later.

As for the type of fracture, the cup-and-cone fracture was more prominent at temperatures in the vicinity of 250 to 300 degrees centigrade. An illustration of this is shown in Figure 25, which is a photomicrograph of the six per cent alloy tested at 230 degrees centigrade. The surface of the specimen is relatively smooth, and most of the elongation resulted from localized necking. As the temperature is increased above 300 degrees centigrade there is a more general reduction in area along the entire length of the specimen before localized necking begins. This is shown in Figure 26, which is a photomicrograph of the six per cent copper-aluminum alloy tested at 382 degrees centigrade. The surface of this specimen appears rougher than that of the specimen shown in Figure 25, even though both specimens were of the same alloy. The reason for this difference in roughness is that the specimen tested at 382 degrees centigrade necked along its entire length considerably

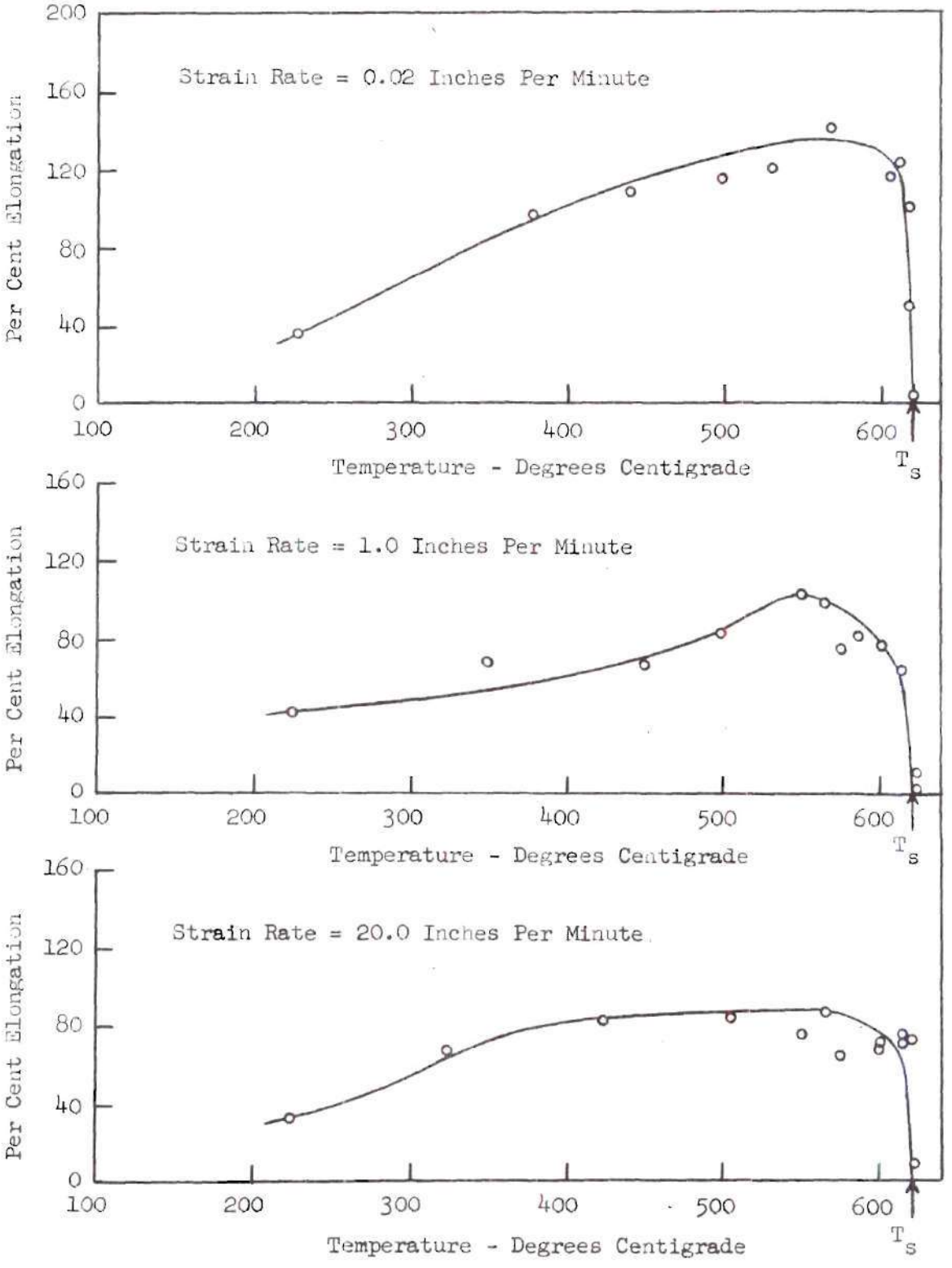

Figure 21. Elongation Versus Temperature for Two Per Cent Copper-Aluminum Alloy. T_s is the Solidus Temperature.

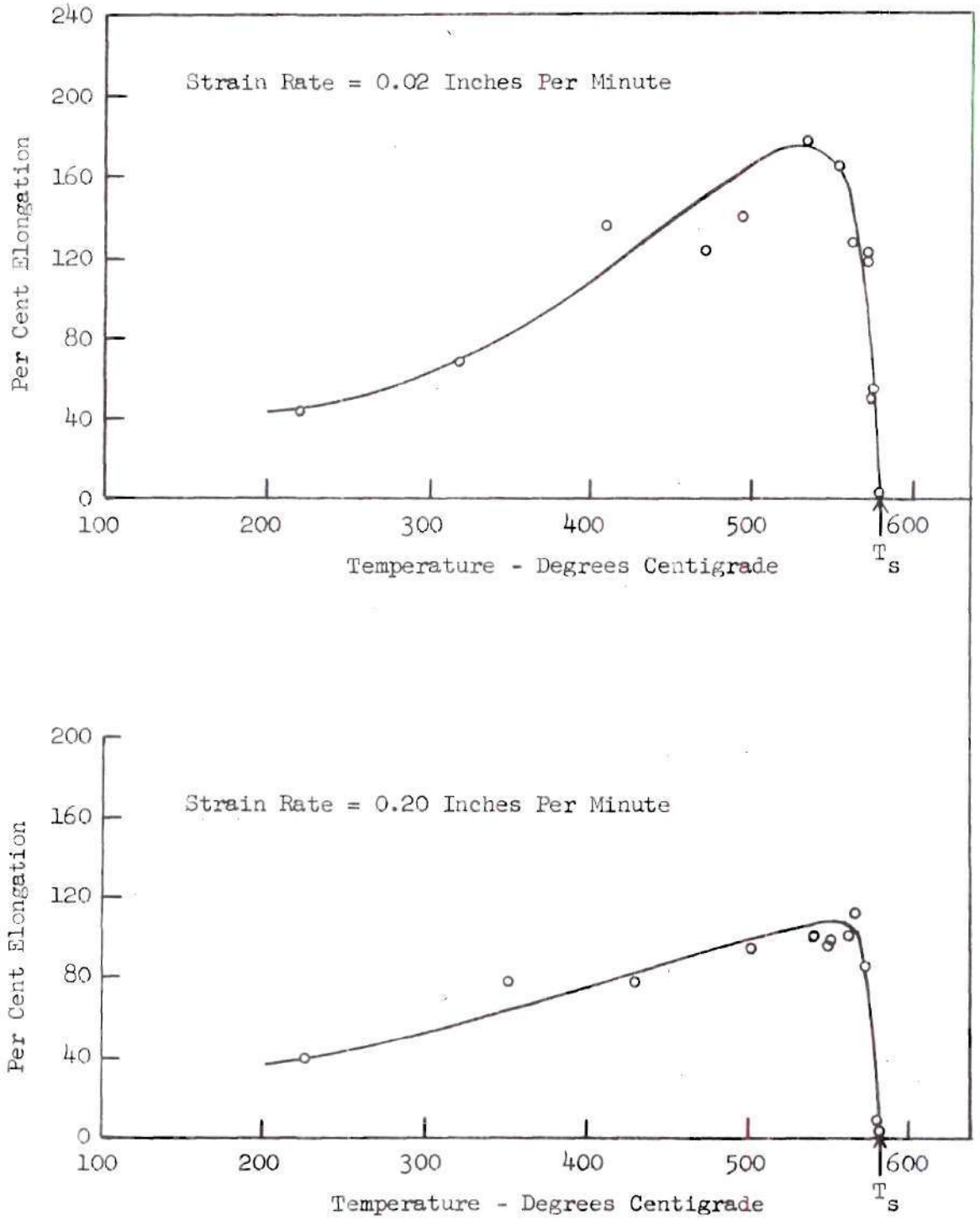

Figure 22. Elongation Versus Temperature for Four Per Cent Copper-Aluminum Alloy. T_s is the Solidus Temperature.

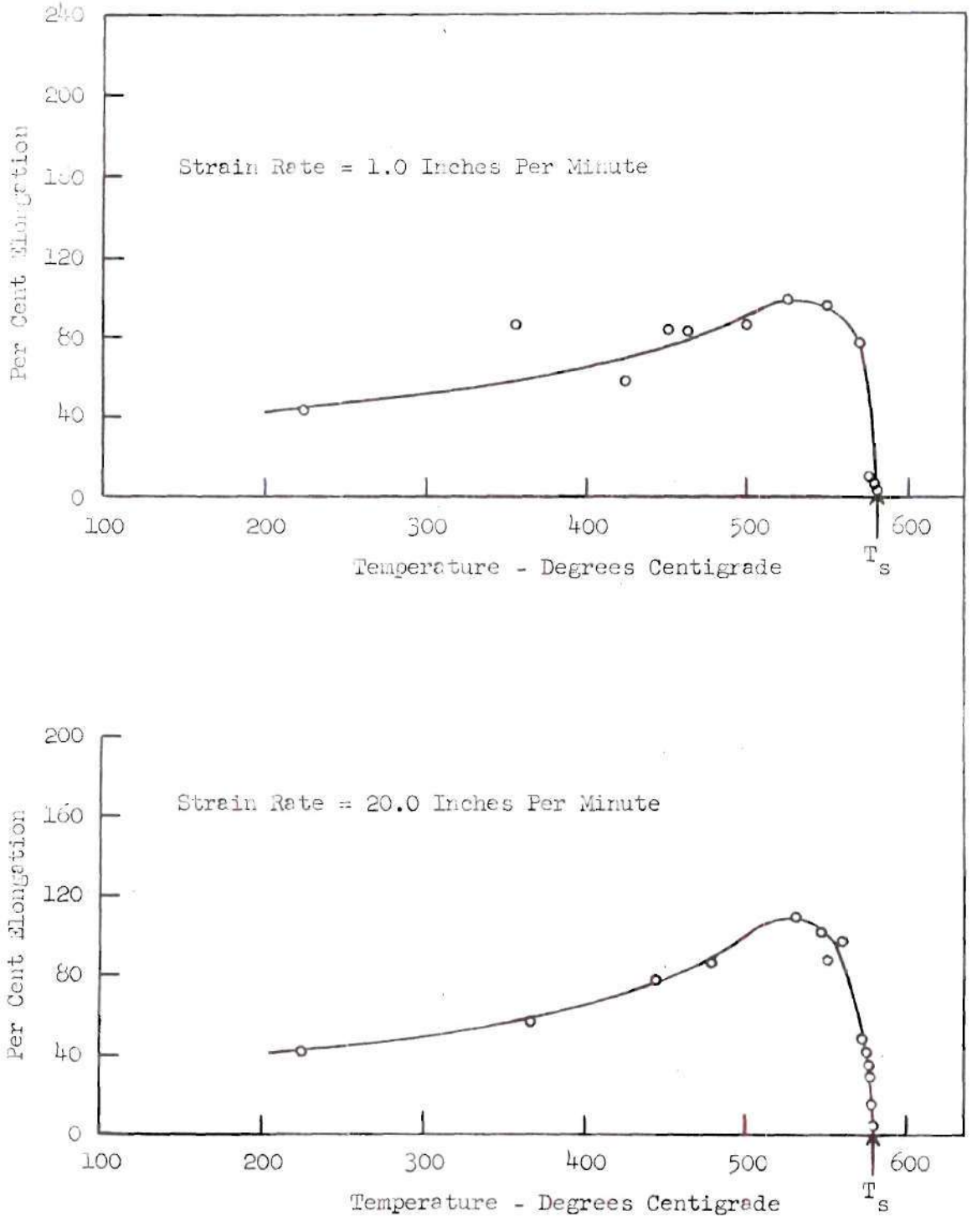

Figure 23. Elongation Versus Temperature for Four Per Cent Copper-Aluminum Alloy. T_s is the Solidus Temperature.

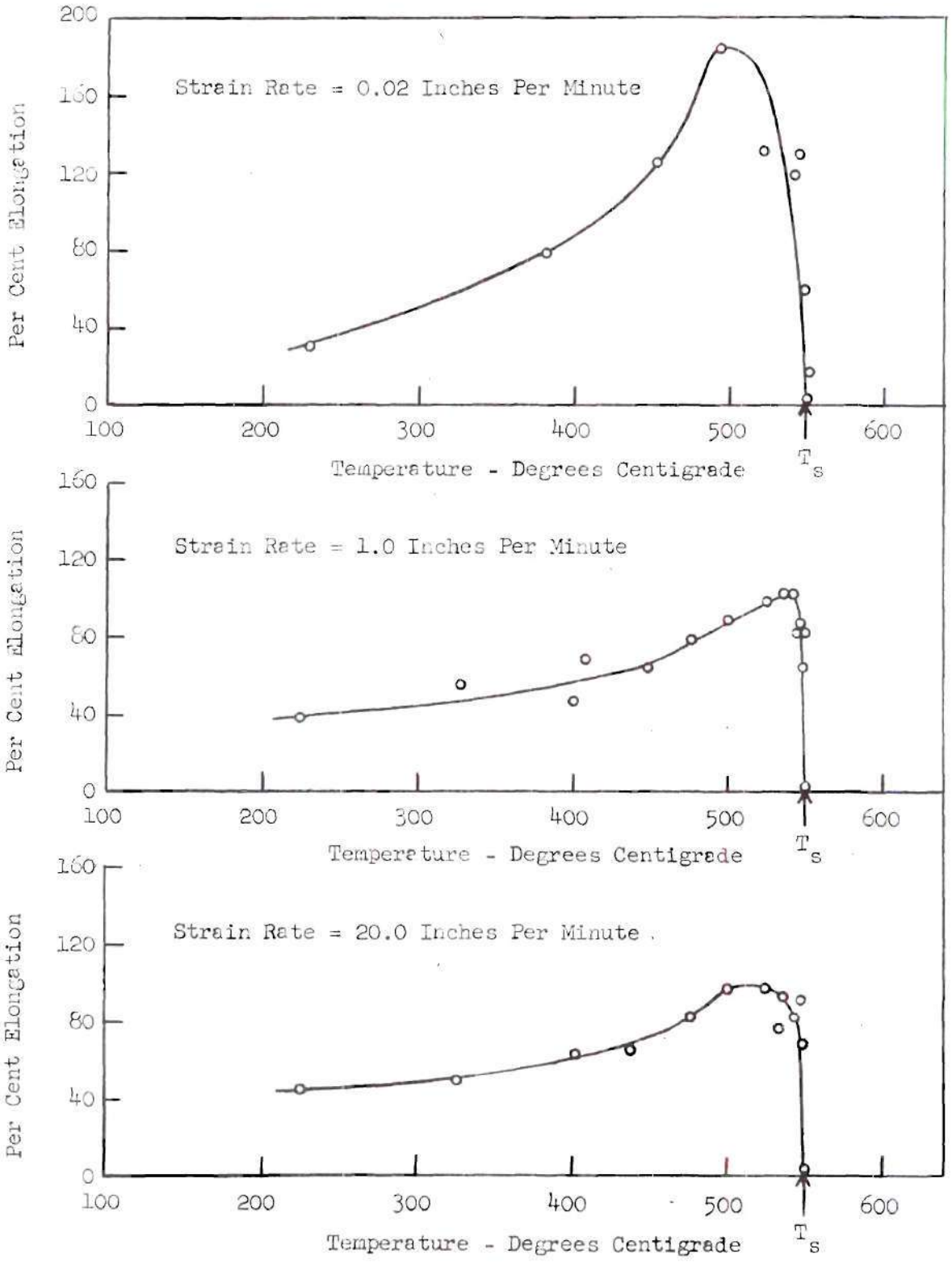

Figure 24. Elongation Versus Temperature for Six Per Cent Copper-Aluminum Alloy. T_s is the Solidus Temperature.

Figure 25. Necked Area of a Six Per Cent Copper Alloy Tested at 230 Degrees Centigrade.

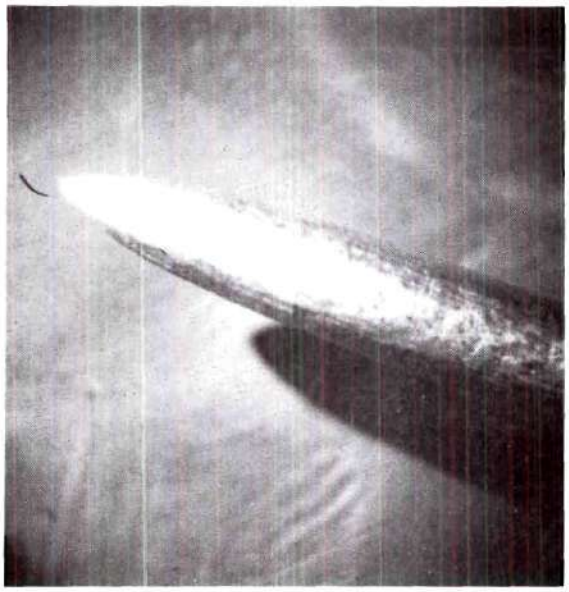

Figure 26. Necked Area of a Six Per Cent Copper Alloy Tested at 382 Degrees Centigrade.

more than the specimen tested at 230 degrees centigrade. Along with the increased roughness, the elongation increased and the area at fracture decreased.

As the temperature is increased from 400 degrees centigrade to the vicinity of 500 degrees centigrade the elongation increases from about 80 per cent to over 180 per cent for the six per cent alloy tested at a strain rate of 0.02 inches per minute. This increase in elongation with an increase in temperature can be interpreted to indicate that recrystallization occurs more rapidly when the temperature is increased. Lesser increases were experienced by the other alloys. The fracture area decreased over this temperature range until the specimen necked down to a point at rupture. Also, there was a greater reduction in area along the entire length of the specimen than occurred at lower temperatures. These two results are illustrated in Figure 27, which shows the six per cent copper-aluminum alloy tested at a temperature of 490 degrees centigrade.

The appearance of the surface of the specimens after they had been tested depended on two factors, the temperature and the per cent copper. The higher the temperature up to a few degrees below the solidus, the rougher the surface was as explained above. The surface was also rougher for the lower per cent copper. This difference in roughness was due to the grain size, which is larger for the lower copper content. The roughness in plastically deformed materials that can be seen by the unaided eye is known as the "orange-peel" effect. In this effect the larger the grain size, the rougher the surface will be. For the specimens tested in this investigation the surfaces were rougher for the larger grain

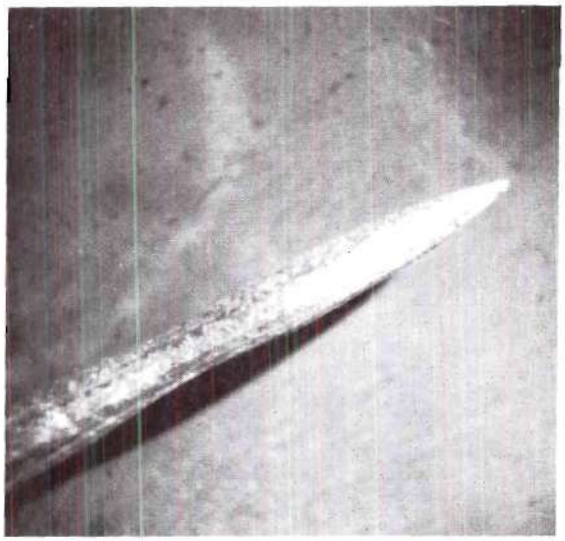

Figure 27. Necked Area of a Six Per Cent Copper Alloy Tested at 490 Degrees Centigrade.

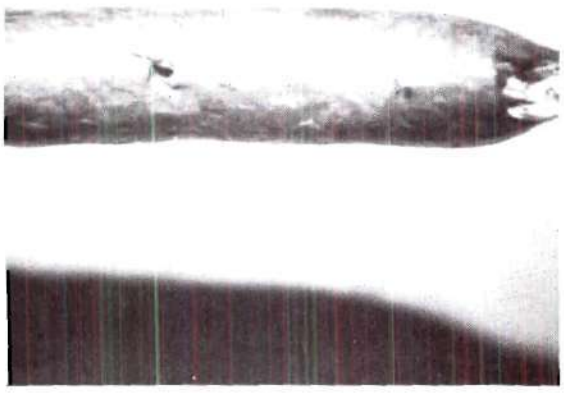

Figure 28. Fracture and Surface of a Four Per Cent Copper Alloy Tested at 579 Degrees Centigrade.

sizes than for the smaller grain sizes.

Failure in the temperature range from room temperature to a few degrees below the solidus occurs by the plastic deformation of the grains. As the temperature approaches the solidus, the ductility starts to decrease and evidence of grain boundary sliding appears. The plastic deformation of the material decreases, and the failure depends more on grain boundary sliding. It is at this stage that the second type of failure begins.

Fracture in the Region of the Solidus

As the solidus temperature is approached, the elongation of the specimens decreases rapidly to very low values and the necking becomes more localized. There was very little uniform reduction in area along the entire length of the specimens of all three alloys. In the two and six per cent alloys the specimens necked locally down to a point at temperatures just below the solidus, but in the four per cent alloy the type of fracture was a combination of both ductile and brittle fracture. Just below the solidus there was considerable evidence of localized necking in the four per cent alloy before the specimens finally failed with brittle fracture. As the solidus temperature was reached, the failure became brittle for all three alloys. The elongation decreased to almost zero, and examination of the specimens revealed no evidence of necking. The failure was completely brittle, and this type of failure is discussed in the next section.

In the type of failure experienced in the region of the solidus the amount of plastic deformation decreases as the temperature increases. Fracture along the grain boundaries increases with increasing temperature.

At first grain boundary sliding occurs, but then grain boundary separation resulting from the presence of a liquid becomes the major form of failure. The type of fracture in the region of the solidus is a combination of ductile grain failure (plastic deformation) and grain boundary separation. An illustration of this is shown in Figure 28, which shows the fracture area and surface of the four per cent alloy tested at 579 degrees centigrade. This temperature is one degree centigrade below the solidus. The localized necking and brittle fracture can be seen clearly.

As the temperature increases above the solidus, the ductile fracture (localized necking and plastic deformation) disappears and brittle intergranular fracture is the only type present. The brittle intergranular fracture consists of grain separation which results from the presence of liquid at the grain boundaries and is the third type of fracture.

Fracture Above the Solidus

Another researcher[12] has investigated fracture in this region, and it has been shown to be a brittle fracture with intergranular failure. This intergranular failure was a result of liquid at the grain boundaries. At lower temperatures in this region some of the individual grain surfaces had a rough appearance while others were smooth. The smooth surfaces occurred where the grain surfaces were completely covered with liquid before fracture, while the rough surfaces indicated that there was solid-to-solid contact between the grains at the time of fracture. However, as the temperature increased above the solidus, this rough fracture area decreased until finally the entire fracture area was smooth. In the upper range of this region there was no evidence of localized necking or plastic deformation. The type of failure was completely brittle.

Elongation of Specimens

Graphs of per cent elongation versus temperature presented in Figures 21 through 24 show that the maximum per cent elongation occurs from 20 to 50 (usually about 50) degrees centigrade below the solidus temperature of the alloys. The ductility of the specimens increases as the temperature is increased up to this range, and then it decreases rapidly to only a few per cent at the solidus temperature. This is in agreement with results obtained by Talbot[12] but does not agree with Novikov.[11] Novikov stated that as the temperature increases the elongation "suddenly drops on passing through the solidus to very low values" and that the maximum elongation occurs at temperatures within a few degrees of the solidus.

The six per cent copper-aluminum alloy had the greatest elongation, followed by the four per cent alloy and then by the two per cent alloy with the least elongation. This increased elongation is contrary to what would be expected because the alloy with the higher copper content had smaller grains. However, it is thought that the specimens with smaller grains are able to deform plastically more before fracture than the larger grains. This increased deformation is due to the softening of the metal that occurs largely through an annealing process, in which the atoms or vacancies of the crystal migrate or diffuse to positions of lower energy, aided by the high thermal energy. Diffusion of these atoms or vacancies seems to take place more easily in the region of highly distorted boundaries than through the crystals themselves. Thus a fine-grained metal, which has more such boundaries than a coarse-grained metal, is subject to more diffusion, and consequently more elongation.

Thus it appears that in this case the ductility increases with a decrease in grain size.[22]

It was also noted that the slower the strain rate, the greater the elongation was. For the strain rate of 0.02 inches per minute, the elongation was much greater than for the other strain rates. In fact, the elongation for the 0.02 inches per minute strain rate was almost twice that obtained at a strain rate of 20.0 inches per minute; and the elongation for the 1.0 inches per minute strain rate was about ten to 15 per cent greater than that for the 20.0 inches per minute strain rate. It is proposed that the reason why specimens tested at slower strain rates elongate more than those tested at high strain rates is that recrystallization has more time to occur at the slower strain rates. Less recrystallization can occur at a given temperature when the strain rate is increased because of the decreased amount of time between the initiation of plastic deformation and fracture. Recrystallization produces grains that are strain free, and as a result the metal is softened and its ductility increased.

Estimated Rough Fracture Area

The aluminum-copper specimens tested by Talbot were examined using a standard Bausch and Lomb StereoZoom Microscope to estimate the amount of rough fracture area that was present after fracture. The rough fracture area occurs where grains had solid-to-solid contact before fracture. As was expected, the per cent rough fracture area for all of the specimens tested at temperatures well below the solidus was 100 per cent. In the region just below the solidus there occasionally

appeared some smooth areas on the fracture surface. The smooth areas occurred mostly in the four per cent alloy and were most prominent at the higher strain rates. To account for the smooth areas in specimens that were tested at temperatures below the solidus it is proposed that these smooth areas are caused by the greater amount of energy present at the higher strain rates. The temperature of the specimen is increased locally where the most resistance to plastic deformation occurs; consequently, the specimen heats up to the solidus temperature in these localized regions and some of the grain boundaries become partially covered with liquid.

As the solidus temperature is reached, the estimated per cent rough fracture area generally falls to a range of from 50 to 75 per cent. For specimens from the same alloy tested at the same temperature but using different strain rates, the rough fracture area is generally greater for the slower strain rates. This is in agreement with the discussion in the previous paragraph, because the specimens tested at higher strain rates appear to have more liquid present at fracture. As the temperature is increased above the solidus, the estimated per cent rough fracture area quickly falls to only a few per cent. This decrease in rough area occurs because more liquid is present at the higher temperature, and the grain boundaries become almost completely covered with liquid. The amount of the grain boundary that becomes covered with liquid at a certain temperature is dependent on the dihedral angle of the alloy. Electron micrographs[12] clearly indicated the difference between the smooth and rough areas. The rough areas appeared to be composed of many small regions that had been plastically deformed, indicating that

solid-to-solid contact existed between grains at the time of fracture. The smooth areas occurred where liquid separated the grains at the time of fracture. The specimens generally lose their coherency about 15 degrees centigrade above the solidus, and at these temperatures the fracture area is usually completely smooth.

The process of liquid spreading over the grain boundaries greatly reduces the maximum stress and percentage elongation. The wetting of the grain boundaries is associated with brittle fracture, which results in lower strength and almost no ductility. The strength decreases as the percentage rough fracture area decreases until there is practically no strength when the grain boundaries are completely covered with liquid. This is also true for the elongation, which decreases to only a few per cent when the estimated rough fracture area decreases below 90 per cent. However, there are a few instances where there is considerable ductility and ultimately brittle fracture. In these cases some grains deform plastically before the grain boundaries become covered with liquid and fail in brittle fracture. This type of failure could be caused by small areas of non-homogeneous material which could account for some specimens having considerable ductility even though the final fracture was mainly brittle.

Uniform Necking

Specimens of all three aluminum-copper alloys tested from 300 degrees centigrade to about 20 degrees centigrade below their solidus temperature exhibited a uniform reduction of area along the entire length of the specimen. This uniform necking occurred even after the

maximum load had been attained and accounts for the large relative elongation present in specimens tested at elevated temperatures. That the uniform necking occurred after maximum load is shown on the stress-strain graphs (See Figure 31 in Appendix A for typical graph) by the fact that most of the elongation occurred after the maximum load had been reached. Following the uniform necking localized necking begins and continues until the necked area draws out to a point and the specimen ruptures.

Nadai and Manjoine[13] mentioned this uniform necking in specimens tested in tension at high temperatures; and they said that it is in contradiction to what is known concerning the behavior of tension-test bars at low temperatures, in which localized necking sets in right after the maximum load is reached. Their stress-strain curves for high temperature tests were similar to the ones obtained in the present investigation. The load increases until the maximum load is obtained, and then the load decreases slowly at an almost constant rate while the specimen is necking uniformly along its entire length. Nadai and Manjoine believed that this flat portion is due to the combined effects of the decrease of the cross-sectional areas of the specimen and of the existence of a pure speed law, which they stated as

$$\sigma = f(\bar{u})$$

or

$$\bar{u} = g(\sigma)$$

where

σ = Stress

$\bar{u}$ = Rate of strain

In the final portion of the stress-strain curve the load falls off rapidly as localized necking sets in.

As stated by Nadai and Manjoine, this uniform necking at elevated temperatures is contrary to what occurs in tensile specimens tested at room temperatures. It has been stated by Richards[22] and Dieter[23] that a real metal undergoes uniform necking when tested at room temperatures until the maximum load is reached. The uniform necking is due to strain-hardening, which tends to increase the load-carrying capacity of the specimen as deformation increases, and to the gradual decrease in the cross-sectional area of the specimen as it elongates. It is generally accepted that localized necking at room temperatures begins at maximum load when the increase in stress due to the decrease in the cross-sectional area of the specimen becomes greater than the increase in the load-carrying abilities of the metal due to strain-hardening. When this condition is reached at some location in the specimen, the plastic strain continues to increase at this location and plastic instability occurs. The deformation becomes highly localized and all further elongation takes place at this location. The result is the formation of a localized neck. As the localized necking continues, the rate of strain-hardening continues to decrease in the necked area; and with the decreasing area the load required to cause further deformation continues to drop.

Plastic instability and localized necking occurred at maximum load in the specimens tested at 225 degrees centigrade. Also plastic instability and localized necking occurred in specimens tested at temperatures above 300 degrees centigrade, but while plastic instability always occurs at maximum load, the localized necking did not start until

after the specimen necked along its entire length. The stress-strain graphs indicated that there was a period of time between the time the maximum load occurred and the time when localized necking began. During this time the specimen continued to reduce uniformly in area along its entire length. This uniform reduction in area, or uniform necking, continues until localized necking begins.

Nadai and Manjoine discussed uniform necking, but no theoretical considerations were given to explain it on a microscopic or macroscopic scale. An explanation will be put forth here to try to explain the physical phenomenon that accounts for the uniform necking that occurred in specimens tested in tension at elevated temperatures. As a first step the uniform necking will be investigated on a microscopic scale, and then these findings will be expanded and used to investigate it on a macroscopic scale.

Plastic deformation in metallic crystals usually occurs by slip or twinning. However, it has been stated that twinning plays only a minor part in the deformation of aluminum and copper.[24] Therefore it has been assumed that slip plays the major roll in the plastic deformation of the alloys used in this investigation. A discussion of the mechanics of slip and critical resolved shear stress is presented in Appendix D.

From the discussion presented in Appendix D it can be seen how plastic deformation occurs in a single crystal. To relate the slip mechanism to the uniform necking that occurred in this investigation, it must be remembered that most crystalline materials are aggregates of many small crystals. These individual crystals are oriented at random

in all possible directions, and consequently the planes and directions of easiest slip vary throughout the specimen. An enlarged sketch of a typical specimen showing a possible random orientation of the grains and their planes of easiest slip is shown in Figure 29. When the tensile stress is applied along the axis of the specimen, the maximum shearing stress will still be on planes at an angle of 45° with the axis. The maximum shearing stress will probably coincide with the planes of easy slip in only a few, if any, of the crystals. Therefore the crystals that are most favorably oriented for slip will appear to be weaker than the others.

After slip has progressed in the crystals with the most favorable orientation, the crystals with the next most favorable orientation for slip begin to yield. The presence of crystal boundaries and adjacent crystals with different orientations restricts the slip in the initially deformed crystals, and slip must begin in these new crystals. However, this requires a greater stress because of the less favorable orientation of the crystals. Once the slip in these crystals is stopped by obstructions, slip must begin in the crystals with the next most favorable orientation. An even larger stress is required. This process continues until the maximum stress is reached. The maximum stress is obtained when the increase in stress due to the decrease in the cross-sectional area of the specimen becomes greater than the increase in the load-carrying abilities of the metal due to strain-hardening. When this condition is reached at some location in a specimen tested at low temperatures, plastic instability occurs and localized necking begins. As the area decreases at this point, the stress increases much faster than

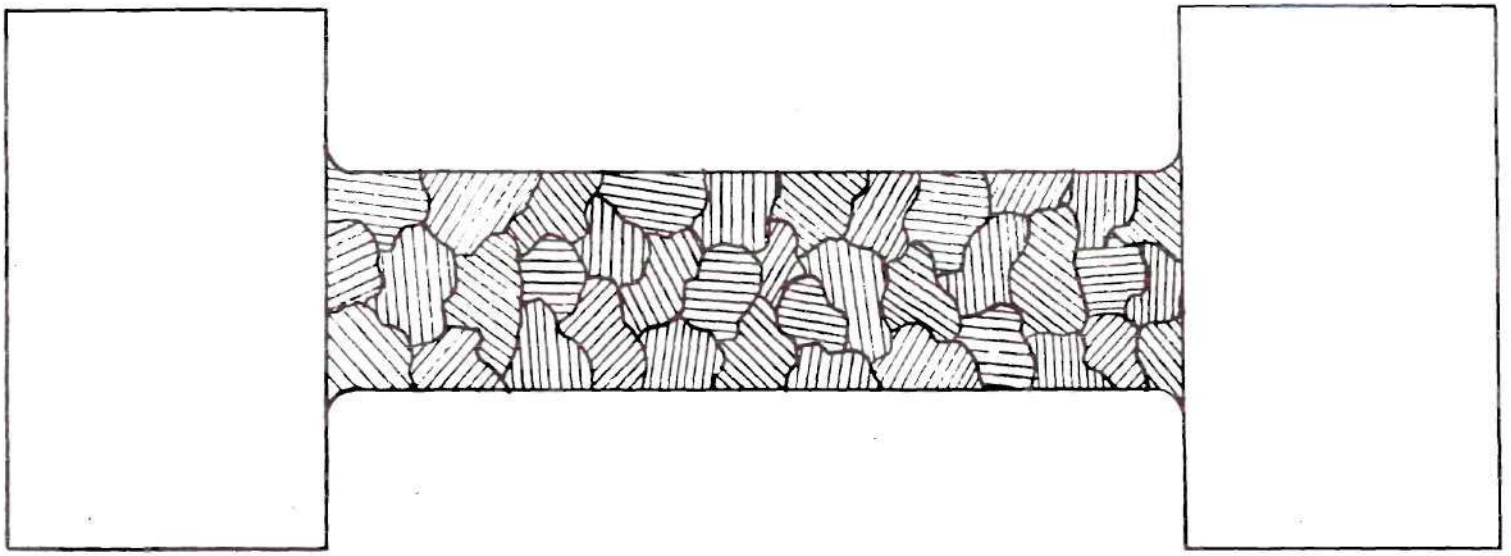

Figure 29. Enlarged Sketch of Tensile Test Specimen Showing Estimated Grain Orientation.

the load-carrying ability increases due to strain-hardening. The cross-sectional area decreases so fast that all the strain occurs here, and no additional strain occurs along the rest of the specimen. Therefore there is no additional reduction in area along the rest of the specimen. The only observable reduction in area occurs at the neck.

However, for the specimens tested in this investigation at temperatures above 300 degrees centigrade localized necking does not occur when the maximum load is reached. The specimen continues to elongate uniformly along its entire length. This process continues until finally localized necking is initiated, and then the specimen necks locally until rupture occurs.

Once past the maximum load, the increase in stress due to the reduction in area is greater than the increase in strength due to strain-hardening. This means that in a constant strain rate test the load will begin to decrease. At high temperatures it is easier for a grain boundary to shift or adjust relative to another boundary when the neighboring grains deform plastically. At temperatures near the solidus the grain boundaries become glissile, and some grain boundary sliding occurs. Also grain boundaries tend to migrate either into the grains having the largest stored energy or because of the force of dislocations that pile up at the boundaries.[25]

While the cross-sectional area of the specimen is reducing, the grain boundaries shift or adjust because of the plastic deformation of the neighboring grains. The high temperature of the specimens makes this shifting or movement of grain boundaries easier; and as it occurs grains that have not been deformed because of unfavorable orientation

translate and rotate until their orientation becomes more favorable for deformation. Figure 30 (a) shows one grain (labeled A) with favorable orientation and another grain (labeled B) with unfavorable orientation. In Figure 30 (b) grain A has deformed, causing grain B to translate and rotate until its orientation becomes more favorable for deformation. Some of these re-oriented grains begins to slip as their critical resolved shear stress is reached. Because of the reduction in the cross-sectional area the total load applied to the specimen required to cause slip has decreased. During this time more grains are being re-oriented by the plastic deformation in neighboring grains and the movement or shifting of grain boundaries. Once they become as favorably oriented as the first grains to slip or when dislocations in the first grains become sessile, these new grains begin to slip. The cross-sectional area of the specimen continues to decrease, and as a result the total load on the specimen required to cause slip continues to decrease. This process occurs along the entire length of the specimen. Grains continue to be re-oriented, and the load required to cause deformation continues to decrease because of the decrease in the cross-sectional area.

In addition to this grain re-orientation the specimens tested at elevated temperatures regardless of the strain rate undergo a certain amount of lattice rearrangement and recovery which contributes to the uniform necking. Guy[26] states that in specimens tested at elevated temperatures the deformed lattice may rearrange itself and eliminate the disturbances produced during deformation by the movement through the lattice of vacancies and interstitial atoms that are created in the deformation process. The vacancies and interstitialcies move from

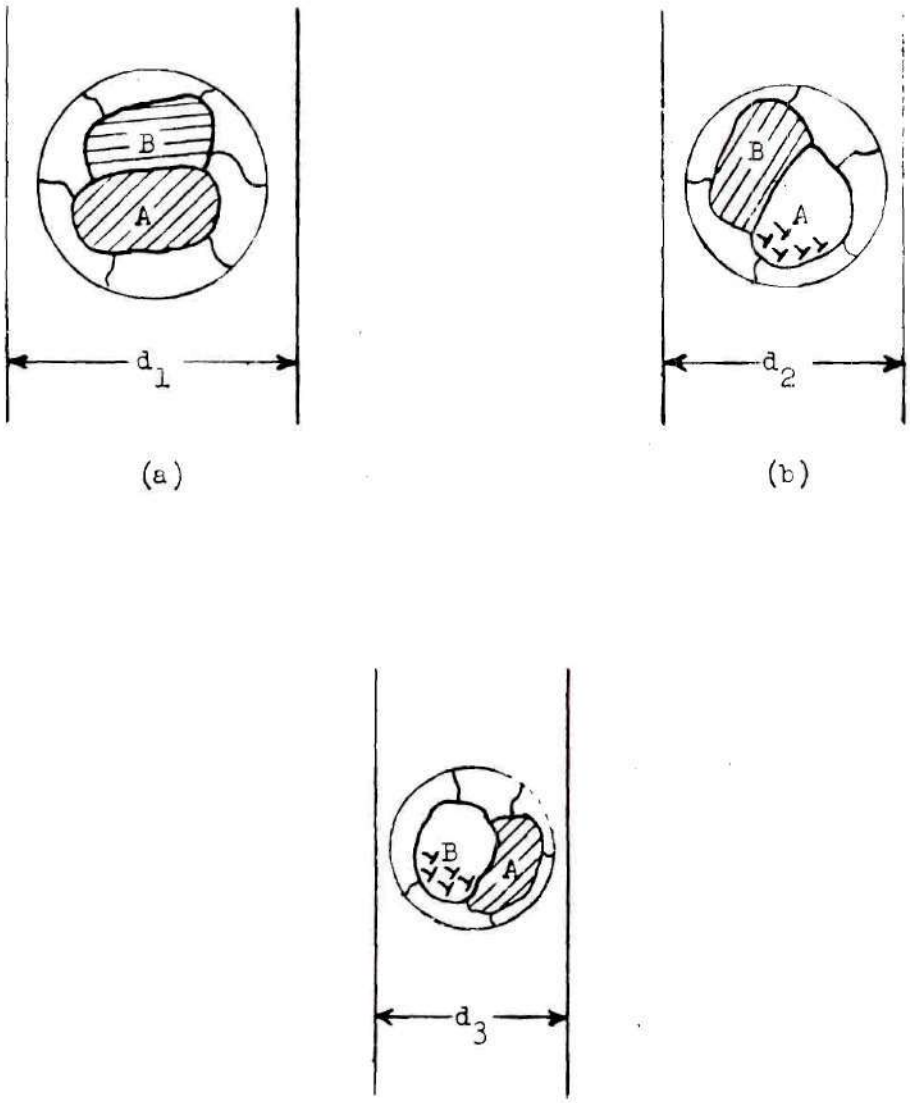

$$d_2 = d_1 - \Delta d_1$$

$$d_3 = d_2 - \Delta d_2$$

Figure 30. Schematic Diagram of Steps Occurring During Uniform Necking.

disturbed regions, where the energy is high, to adjacent portions of the lattice where they can aid in forming a structure of higher perfection and lower energy. Also some rearrangement of the lattice may occur by the climb of a dislocation in which a vacancy diffuses to a dislocation and causes it to climb to the next higher slip plane.

Uniform necking was much more prominent at the lower strain rates than at the higher strain rates. In the tests which took over one hour to run the process of recrystallization can occur many times. Figure 30 (c) shows grain A which has been recrystallized.

Recrystallization occurs by the formation of nuclei preferentially in areas of high lattice distortion, such as near grain boundaries, deformation bands, or inclusions. In regions of high lattice distortion the strain-energy is high, and recrystallization nuclei form. These nuclei, which have a lower strain-energy than the surrounding matrix, form by the diffusion of atoms and vacancies to positions of lower energy. The rate of vacancy diffusion is quite rapid, and because of this high rate of diffusion the grain boundaries migrate quickly. Since the strain-energy of these nuclei is lower than the strain-energy of the surrounding matrix, the grain boundaries continue to migrate into this surrounding matrix by the diffusion of atoms and vacancies. Growth of each nucleus by boundary migration with the subsequent elimination of dislocations continues until mutual interference prevents further growth. The process is then repeated, producing more recrystallized grains.

These recrystallized grains are strain-free; and the metal is thereby softened, its ductility increased, and its strength lowered. The process of grains recrystallizing occurs along the entire length

of the specimen, and slip occurs first in these recrystallized grains that have the most favorable orientation. During this time more grains recrystallize as the process continues, and the load required to cause deformation decreases because the cross-sectional area decreases. Finally localized necking begins at a point where the cross-sectional area decreases faster than the strength increases because of strain-hardening. All further strain occurs in the localized area until rupture occurs.

It is believed that uniform necking results from a combination of the processes discussed above. At the slow strain rates uniform necking is much greater than at high strain rates, and it is proposed that this uniform necking is caused by a combination of grain boundary movement, recovery, and recrystallization. At the higher strain rates there is not as much time for recrystallization to occur, so therefore the uniform necking consists mainly of grain boundary movement, recovery, and only a limited amount of recrystallization. As a result the total elongation is less.

CHAPTER V

CONCLUSIONS AND RECOMMENDATIONS

An experimental investigation of the fracture mechanism of three aluminum-copper alloys in the region of the solidus temperature has been carried out. From the results of this investigation the following conclusions can be made:

1. The stress to fracture versus temperature curves for the aluminum-copper alloy system in the region of the solidus are similar to curves obtained for other aluminum alloy systems by other investigators.

2. The addition of more copper increases the strength and relative elongation of the alloy system.

3. An increase in the strain rate increases the strength but decreases the relative elongation in the region below the solidus. Above the solidus increasing the strain rate decreases the strength.

4. Between 200 degrees centigrade and the solidus temperature there are two types of fracture. The first occurs well below the solidus and consists of plastic deformation. The second occurs in the region of the solidus and consists of both plastic deformation and intergranular failure (grain boundary separation).

5. The ductility of the alloy system increases as the temperature is increased to 20 to 50 (usually about 50) degrees centigrade below the solidus. Then the elongation decreases to only a few per cent at or just above the solidus temperature.

6. The estimated rough fracture area is dependent upon the temperature of the specimen. It is 100 per cent below the solidus and decreases to zero as the temperature increases to 10 to 15 degrees centigrade above the solidus.

7. Specimens tested at temperatures from 300 degrees centigrade up to the solidus temperature exhibit a uniform reduction in area along the entire length of the specimen even after the maximum load has been attained. This uniform reduction of area results from a combination of the work hardening, recovery, and recrystallization processes.

The following recommendations are made as a logical extension of the work which has been presented here:

1. Carry out investigations similar to the present work on alloys of aluminum and other elements such as magnesium, manganese, zinc, etc. to see if similar results are obtained.

2. Make a more detailed study of the effect of strain rates on the type of failure present within plus or minus a few degrees of the solidus temperature.

3. Carry out investigations in a range of temperatures from 75 degrees centigrade below the solidus to the solidus and determine the reason for maximum elongation occurring 20 to 50 degrees centigrade below the solidus.

4. Perform experiments using alloys with additional copper to see if there is a limit to the amount of copper that can be added feasibly to increase the strength and ductility of the alloy.

5. Perform experiments on ternary alloys to determine what effect the addition of a third element has on the properties of alloys

in the region of the solidus.

6. Try to correlate the data presented in this work to see if mathematical relationships exist between the stress, per cent copper, temperature and rate of straining.

7. Perform experiments to determine the time required for recrystallization to occur at temperatures in the region just below the solidus.

8. Perform experiments to determine the self-diffusion rate of aluminum and aluminum alloys at and near the solidus temperature.

9. Carry out tests to determine true stress versus true strain curves for materials that exhibit uniform necking at elevated temperatures.

APPENDICES

APPENDIX A

CALCULATION AND TABULATION OF RESULTS

The experimental results obtained for each specimen are presented in Tables 5 through 14. These results were obtained using the experimental equipment and procedure described in Chapters II and III. The method for calculating each item in the tables of this section is explained below. A typical graph is shown in Figure 31 to aid in this explanation.

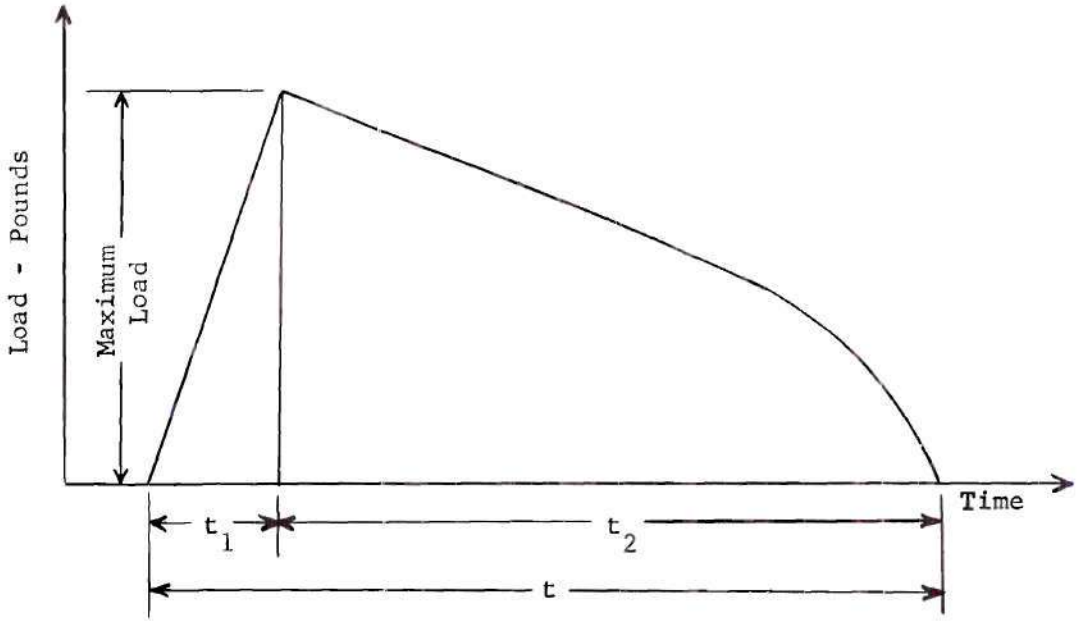

Figure 31. Typical Graph For Specimen

1. The stress in pounds per square inch is determined by dividing the load in pounds by the cross-sectional area of the specimen.

$$\sigma = P/A \quad lb/in^2$$

where

σ = Stress, lb/in^2

P = Load, lbs

A = Cross-sectional area, in^2

2. The total strain is the total elongation of the specimen divided by its original length.

$$\epsilon = \dot{\epsilon}t/\ell \text{ in/in}$$

where

ϵ = Total strain, in/in

$\dot{\epsilon}$ = Strain rate, in/min

t = Total time of test, min

ℓ = Original length of test specimen, in

3. The strain to maximum stress is the elongation to maximum stress divided by the original length of the specimen.

$$\epsilon_1 = \dot{\epsilon}t_1/\ell \text{ in/in}$$

where

ϵ_1 = Strain to maximum stress, in/in

$\dot{\epsilon}$ = Strain rate, in/min

t_1 = Time to maximum stress, min

ℓ = Original length of test specimen, in

4. The strain from maximum stress to fracture is the elongation from maximum stress to fracture divided by the original length of the specimen.

$$\epsilon_2 = \dot{\epsilon} t_2 / \ell \text{ in/in}$$

where

ϵ_2 = Strain from maximum stress to fracture, in/in

$\dot{\epsilon}$ = Strain rate, in/min

t_2 = Time from maximum stress to fracture, min

ℓ = Original length of test specimen, in

5. The time to maximum stress, time from maximum stress to fracture, and total time are measured directly from the graph.

Table 5. Experimental Data for the 2 Per Cent Copper Alloy Tested at a Strain Rate of 0.02 Inches Per Minute.[12]

Specimen Number	Temp °C	Per Cent Liquid	Stress psi	Total Strain in/in x100	Strain to Max Stress in/in x100	Strain from Max Stress to Fracture in/in x100	Time to Max Stress min	Total Time min	Est Per Cent Rough Fracture Surface
2-16	230	0	4500	35.6	3.72	31.9	1.900	--	100
2-15	379	0	1800	95.0	0.667	94.3	0.350	--	100
2-14	441	0	1125	107.0	0.720	106.3	0.550	--	100
2-12	500	0	680	113.0	0.820	112.2	0.500	--	100
2-13	532	0	550	118.8	0.380	118.4	0.350	--	100
2-11	568	0	410	139.0	0.450	138.5	1.000	--	100
2-10	606	0	280	113.8	0.580	113.2	0.800	--	100
2-9	613	0	250	121.0	0.320	120.7	0.500	--	100
2-7	618	0	215	48.1	0.310	47.8	0.300	--	25
2-2	619.5	0	280	98.2	0.720	97.5	0.750	--	100
2-5	622	0.8	240	1.80	0.360	1.44	0.250	0.750	50
2-3	625	2.6	150	0.36	0.153	0.21	0.180	0.230	50

(Continued)

Table 5. Experimental Data for the 2 Per Cent Copper Alloy Tested at a Strain Rate of 0.02 Inches Per Minute.[12] (Continued)

Specimen Number	Temp °C	Per Cent Liquid	Stress psi	Total Strain in/in x100	Strain to Max Stress in/in x100	Strain from Max Stress to Fracture in/in x100	Time to Max Stress min	Total Time min	Est Per Cent Rough Fracture Surface
2-4	630	6.8	12.5	0.36	0.150	0.21	0.0125	0.025	0
2-8	632.5	9.7	35	0.90	0.36	0.54	0.125	0.250	2
2-1	634	12.7	0	--	--	--	--	--	0

Table 6. Experimental Data for the 2 Per Cent Copper Alloy Tested at a Strain Rate of 1.0 Inches Per Minute.

Specimen Number	Temp °C	Per Cent Liquid	Stress psi	Total Strain in/in x100	Strain to Max Stress in/in x100	Strain from Max Stress to Fracture in/in x100	Time to Max Stress min	Total Time min	Est Per Cent Rough Fracture Surface
2-84	225	0	11600	40.9	8.47	32.4	0.0940	0.454	100
2-85	350	0	4178	66.7	4.61	62.1	0.0520	0.752	100
2-68	450	0	2415	64.6	4.56	60.0	0.0500	0.708	100
2-74	498	0	1808	80.9	7.55	73.4	0.0820	0.879	100
2-67	550	0	1390	100.8	12.00	88.8	0.134	1.130	100
2-83	564	0	1247	96.0	8.64	87.4	0.0970	1.077	100
2-69	575	0	1123	72.4	12.00	60.4	0.1350	0.814	100
2-86	586	0	1000	79.1	5.24	73.9	0.0590	0.890	100
2-71	600	0	971	75.3	4.74	70.6	0.0530	0.843	100
2-72	614	0	789	62.6	11.40	51.2	0.1280	0.702	100
2-43*	623	1.4	700	70.2	0.74	69.5	0.0220	0.160	100
2-44*	625	2.5	495	8.98	0.67	8.31	0.0220	0.100	50

(Continued)

Table 6. Experimental Data for the 2 Per Cent Copper Alloy Tested at a Strain Rate of 1.0 Inches Per Minute. (Continued)

Specimen Number	Temp °C	Per Cent Liquid	Stress psi	Total Strain in/in x100	Strain to Max Stress in/in x100	Strain from Max Stress to Fracture in/in x100	Time to Max Stress min	Total Time min	Est Per Cent Rough Fracture Surface
2-51*	625	2.5	330	1.81	0.54	1.27	0.0100	0.020	15
2-52*	627	4.0	80	3.64	0.55	3.09	0.0150	0.030	10
2-46*	627.5	4.5	150	2.28	0.55	1.73	0.0100	0.030	20
2-45*	631	7.9	60	1.82	0.40	1.42	0.0100	0.030	2

* - Reference 12.

Table 7. Experimental Data for the 2 Per Cent Copper Alloy Tested at a Strain Rate of 20.0 Inches Per Minute.

Specimen Number	Temp °C	Per Cent Liquid	Stress psi	Total Strain in/in x100	Strain to Max Stress in/in x100	Strain from Max Stress to Fracture in/in x100	Time to Max Stress min	Total Time min	Est Per Cent Rough Fracture Surface
2-82	225	0	14400	31.6	14.2	17.4	0.00808	0.018	100
2-75	325	0	8710	66.8	10.7	56.1	0.00600	0.038	100
2-77	424	0	4522	81.6	14.5	67.1	0.00825	0.046	100
2-79	505	0	3000	83.0	12.9	70.1	0.00733	0.047	100
2-76	550	0	2439	74.8	11.5	63.3	0.00642	0.042	100
2-90	565	0	2322	85.5	11.5	74.0	0.00650	0.048	100
2-78	574	0	2143	63.1	11.9	51.2	0.00658	0.035	100
2-80	599	0	1856	66.4	11.5	54.9	0.00642	0.037	100
2-87	600	0	1857	69.9	14.7	55.2	0.00825	0.040	100
2-88	614	0	1710	75.4	10.9	64.5	0.00600	0.042	100
2-81	615	0	1601	70.7	10.2	60.5	0.00558	0.039	100
2-89	618	0	1531	71.0	15.7	55.3	0.00867	0.039	100

(Continued)

Table 7. Experimental Data for the 2 Per Cent Copper Alloy Tested at a Strain Rate of 20.0 Inches Per Minute. (Continued)

Specimen Number	Temp °C	Per Cent Liquid	Stress psi	Total Strain in/in x100	Strain to Max Stress in/in x100	Strain from Max Stress to Fracture in/in x100	Time to Max Stress min	Total Time min	Est Per Cent Rough Fracture Surface
2-58*	621	0.3	1085	8.35	4.02	4.33	0.00250	0.005	75
2-53*	623	1.4	1170	24.0	7.36	16.64	0.00340	0.015	95
2-56*	624	2.0	132.5	3.18	0.70	2.48	0.00140	0.004	20
2-60*	625	2.6	100	2.70	1.00	1.70	0.00150	0.004	15
2-57*	626	2.8	41.5	2.50	1.00	1.50	0.00150	0.004	10
2-59*	628	5.0	83.5	1.45	1.00	0.45	0.00200	0.006	5

* - Reference 12.

Table 8. Experimental Data for the 4.12 Per Cent Copper Alloy Tested at a Strain Rate of 0.02 Inches Per Minute.

Specimen Number	Temp °C	Per Cent Liquid	Stress psi	Total Strain in/in x100	Strain to Max Stress in/in x100	Strain from Max Stress to Fracture in/in x100	Time to Max Stress min	Total Time min	Est Per Cent Rough Fracture Surface
4-138	220	0	10440	45.5	7.45	38.1	4.10	25.18	100
4-139	318	0	4390	64.0	2.69	61.3	1.50	35.6	100
4-16	411	0	2025	136.0	0.37	135.6	0.250	--	100
4-1	471	0	1400	122.0	0.30	121.7	0.150	--	100
4-17	495	0	975	140.0	0.45	139.5	0.500	--	100
4-2	535	0	700	176.5	0.40	176.1	0.100	--	100
4-7	554	0	725	164.0	0.72	163.3	--	--	100
4-5	562	0	590	126.3	0.29	126.0	0.225	--	100
4-14	572	0	550	121.0	0.39	120.6	0.200	--	100
4-9	572	0	525	118.0	1.27	116.7	0.800	--	100
4-13	579	0	410	48.6	0.91	47.7	0.500	--	100
4-11	580	0.4	410	55.0	0.45	54.5	0.250	--	90

(Continued)

Table 8. Experimental Data for the 4 Per Cent Copper Alloy Tested at a Strain Rate of 0.02 Inches Per Minute.[12] (Continued)

Specimen Number	Temp °C	Per Cent Liquid	Stress psi	Total Strain in/in x100	Strain to Max Stress in/in x100	Strain from Max Stress to Fracture in/in x100	Time to Max Stress min	Total Time min	Est Per Cent Rough Fracture Surface
4-10	584	1.5	410	1.40	0.18	1.22	0.400	0.90	40
4-15	587	2.4	390	2.50	0.80	1.70	1.500	1.10	75
4-12	589	3.1	310	2.30	0.29	2.01	0.225	0.25	20
4-18	590	3.5	140	2.14	0.23	1.91	0.600	1.10	--
4-6	594	4.8	0	--	--	--	--	--	0
4-19	595	5.2	30	1.11	0.18	0.93	0.200	0.50	1

Table 9. Experimental Data for the 4 Per Cent Copper Alloy Tested at a Strain Rate of 0.20 Inches Per Minute.

Specimen Number	Temp °C	Per Cent Liquid	Stress psi	Total Strain in/in x100	Strain to Max Stress in/in x100	Strain from Max Stress to Fracture in/in x100	Time to Max Stress min	Total Time min	Est Per Cent Rough Fracture Surface
4-129	226	0	14325	39.4	7.64	31.8	0.425	2.18	100
4-128	352	0	4460	78.2	2.36	75.8	0.130	4.30	100
4-106	430	0	2201	77.0	11.90	65.1	0.720	4.66	100
4-125	500	0	1758	94.9	1.24	93.7	0.070	5.34	100
4-117	540	0	1520	100.7	0.857	99.8	0.048	5.64	100
4-103	549	0	1351	95.7	1.23	94.5	0.075	5.84	100
4-92	550	0	1394	98.0	1.16	96.8	0.064	5.41	100
4-118	561	0	1133	100.6	0.850	99.7	0.047	5.57	100
4-124	565	0	1125	112.0	0.536	111.4	0.030	6.27	100
4-119	571	0	965	85.3	0.638	84.7	0.034	4.75	100
4-137	575	0	1014	3.05	1.000	2.05	0.050	0.213	50
4-136	577	0	1103	8.35	0.540	7.81	0.030	0.466	50

(Continued)

Table 9. Experimental Data for the 4 Per Cent Copper Alloy Tested at a Strain Rate of 0.20 Inches Per Minute. (Continued)

Specimen Number	Temp °C	Per Cent Liquid	Stress psi	Total Strain in/in x100	Strain to Max Stress in/in x100	Strain from Max Stress to Fracture in/in x100	Time to Max Stress min	Total Time min	Est Per Cent Rough Fracture Surface
4-120	578	0	905	3.26	0.990	2.26	0.055	0.180	40
4-22*	580	0	780	24.4	0.904	23.5	0.100	1.40	75
4-26*	581	0.6	850	4.06	0.741	3.32	0.030	0.10	25
4-23*	587	2.4	650	1.20	0.282	0.92	0.020	0.05	5
4-24*	590	3.5	565	1.70	0.264	1.44	0.030	0.10	5
4-25*	594	4.8	215	1.70	0.441	1.26	0.050	0.10	3
4-27*	597	6.0	215	0.80	0.260	0.54	0.020	0.05	2

* - Reference 12.

Table 10. Experimental Data for the 4 Per Cent Copper Alloy Tested at a Strain Rate of 1.0 Inches Per Minute.

Specimen Number	Temp °C	Per Cent Liquid	Stress psi	Total Strain in/in x100	Strain to Max Stress in/in x100	Strain from Max Stress to Fracture in/in x100	Time to Max Stress min	Total Time min	Est Per Cent Rough Fracture Surface
4-126	226	0	15650	42.8	9.10	33.7	0.100	0.470	100
4-127	356	0	5050	85.0	4.09	80.9	0.045	0.935	100
4-104	425	0	3220	56.2	4.32	51.9	0.052	0.676	100
4-100	451	0	3086	82.6	4.00	78.6	0.044	0.908	100
4-90	463	0	3158	80.7	3.31	77.4	0.037	0.902	100
4-99	500	0	2540	85.4	6.88	78.5	0.078	0.968	100
4-93	525	0	2328	96.8	8.62	88.2	0.097	1.089	100
4-91	550	0	1743	94.0	7.23	86.8	0.080	1.040	100
4-102	570	0	1752	75.2	0.409	74.8	0.005	0.920	100
4-121	575	0	1723	9.84	0.890	8.95	0.010	0.110	25
4-123	578	0	1676	7.53	0.908	6.62	0.010	0.083	25
4-135	579	0	1393	5.87	0.990	4.88	0.011	0.065	15

(Continued)

Table 10. Experimental Data for the 4 Per Cent Copper Alloy Tested at a Strain Rate of 1.0 Inches Per Minute. (Continued)

Specimen Number	Temp °C	Per Cent Liquid	Stress psi	Total Strain in/in x100	Strain to Max Stress in/in x100	Strain from Max Stress to Fracture in/in x100	Time to Max Stress min	Total Time min	Est Per Cent Rough Fracture Surface
4-33*	581	0.6	1450	7.50	0.189	7.31	0.010	0.105	95
4-34*	584	1.5	1225	3.00	0.816	2.18	0.010	0.030	25
4-35*	587	2.4	865	2.24	0.595	1.65	0.010	0.030	15
4-36*	589	3.1	60	1.99	0.299	1.70	0.005	0.020	2
4-37*	589	3.1	120	1.40	0.505	0.90	0.007	0.015	5
4-38*	591	3.8	45	2.00	0.500	1.50	0.007	0.015	2
4-39*	593	4.5	60	2.08	0.520	1.56	0.006	0.020	0

* - Reference 12.

Table 11. Experimental Data for the 4 Per Cent Copper Alloy Tested at a Strain Rate of 20.0 Inches Per Minute.

Specimen Number	Temp °C	Per Cent Liquid	Stress psi	Total Strain in/in x100	Strain to Max Stress in/in x100	Strain from Max Stress to Fracture in/in x100	Time to Max Stress min	Total Time min	Est Per Cent Rough Fracture Surface
4-114	225	0	18320	41.8	16.5	25.3	0.01017	0.0258	100
4-101	367	0	6850	56.7	13.8	42.9	0.00750	0.0309	100
4-108	445	0	5000	76.9	10.0	66.9	0.00567	0.0434	100
4-107	479	0	4478	86.1	15.9	70.2	0.00883	0.0478	100
4-109	531	0	4208	108.0	11.4	96.6	0.00642	0.0606	100
4-134	546	0	3392	100.4	11.4	89.0	0.00642	0.0564	100
4-130	550	0	3269	86.5	11.5	75.0	0.00642	0.0481	100
4-131	560	0	2956	96.0	10.0	86.0	0.00550	0.0533	100
4-112	572	0	2955	49.0	12.4	36.6	0.00683	0.0270	50
4-110	574	0	2722	40.7	12.3	28.4	0.00683	0.0226	50
4-115	576	0	3050	34.8	10.7	24.1	0.00667	0.0216	50
4-132	576	0	2428	29.0	12.3	16.7	0.00683	0.0161	50

(Continued)

Table 11. Experimental Data for the 4 Per Cent Copper Alloy Tested at a Strain Rate of 20.0 Inches Per Minute. (Continued)

Specimen Number	Temp °C	Per Cent Liquid	Stress psi	Total Strain in/in x100	Strain to Max Stress in/in x100	Strain from Max Stress to Fracture in/in x100	Time to Max Stress min	Total Time min	Est Per Cent Rough Fracture Surface
4-133	577	0	1812	15.5	5.66	9.8	0.00317	0.0087	30
4-113	578	0	915	4.90	1.64	3.26	0.00092	0.0028	25
4-43*	581	0.6	400	5.00	1.35	3.65	0.00067	0.0026	5
4-44*	583	1.2	275	3.18	1.13	2.05	0.00067	0.0020	15
4-45*	586	2.1	83	2.80	1.13	1.67	0.00055	0.0015	3
4-46*	589	3.1	75	2.76	1.13	1.65	0.00056	0.0019	2
4-47*	591	3.8	75	2.72	1.13	1.59	0.00056	0.0017	1
4-49*	593.5	4.7	25	2.18	1.13	1.05	0.00056	0.0013	1

* - Reference 12.

Table 12. Experimental Data for the 6 Per Cent Copper Alloy Tested at a Strain Rate of 0.02 Inches Per Minute.[12]

Specimen Number	Temp °C	Per Cent Liquid	Stress psi	Total Strain in/in x100	Strain to Max Stress in/in x100	Strain from Max Stress to Fracture in/in x100	Time to Max Stress min	Total Time min	Est Per Cent Rough Fracture Surface
6-2	230	0	15250	30.6	2.88	27.7	2.00	--	100
6-1	382	0	2200	79.1	1.10	78.0	0.60	--	100
6-3	453	0	1375	124.6	1.075	123.5	0.60	--	100
6-4	494	0	1200	183.0	2.09	180.9	1.20	--	100
6-14	521	0	925	129.5	1.00	128.5	0.70	--	100
6-6	541	0	960	118.0	1.001	117.0	0.55	--	100
6-15	545	0	750	128.5	0.59	127.9	0.30	--	100
6-16	548	1.5	720	59.5	0.873	58.6	0.50	--	60
6-12	550	1.6	620	2.00	0.545	1.45	0.60	1.00	25
6-8	551	1.7	615	16.4	0.911	15.5	0.55	4.25	50
6-5	552	1.99	580	2.00	0.5	1.50	0.30	0.50	35
6-9	555	2.4	150	0.80	0.225	0.575	0.30	0.50	15

(Continued)

Table 12. Experimental Data for the 6 Per Cent Copper Alloy Tested at a Strain Rate of 0.02 Inches Per Minute,[12] (Continued)

Specimen Number	Temp °C	Per Cent Liquid	Stress psi	Total Strain in/in x100	Strain to Max Stress in/in x100	Strain from Max Stress to Fracture in/in x100	Time to Max Stress min	Total Time min	Est Per Cent Rough Fracture Surface
6-7	556	2.6	160	1.12	0.32	0.80	0.30	0.70	10
6-10	560	3.4	170	0.73	0.224	0.505	0.35	0.45	5
6-11	562	3.9	100	2.23	0.49	1.74	0.30	0.45	0
6-13	564	4.3	0	--	--	--	--	--	2

Table 13. Experimental Data for the 6 Per Cent Copper Alloy Tested at a Strain Rate of 1.0 Inches Per Minute.

Specimen Number	Temp °C	Per Cent Liquid	Stress psi	Total Strain in/in x100	Strain to Max Stress in/in x100	Strain from Max Stress to Fracture in/in x100	Time to Max Stress min	Total Time min	Est Per Cent Rough Fracture Surface
6-93	225	0	16940	38.3	7.14	31.2	0.0780	0.418	100
6-94	327	0	7420	55.7	5.36	50.3	0.0600	0.624	100
6-70	400	0	4456	46.2	0.80	45.4	0.0090	0.518	100
6-68	407	0	4465	68.0	0.98	67.0	0.0110	0.763	100
6-71	447	0	3691	63.9	1.42	62.5	0.0160	0.718	100
6-74	475	0	3313	78.1	1.42	76.7	0.0160	0.878	100
6-72	499	0	3170	88.0	1.24	86.7	0.0140	0.993	100
6-69	524	0	3084	98.5	1.07	97.4	0.0120	1.108	100
6-76	535	0	2945	102.6	0.89	101.7	0.0100	1.147	100
6-97	540	0	2515	102.2	1.79	100.4	0.0200	1.142	100
6-73	543	0	2828	81.4	0.80	80.6	0.0090	0.917	100
6-92	545	0	2800	87.5	0.80	86.7	0.0090	0.984	100

(Continued)

Table 13. Experimental Data for the 6 Per Cent Copper Alloy Tested at a Strain Rate of 1.0 Inches Per Minute. (Continued)

Specimen Number	Temp °C	Per Cent Liquid	Stress psi	Total Strain in/in x100	Strain to Max Stress in/in x100	Strain from Max Stress to Fracture in/in x100	Time to Max Stress min	Total Time min	Est. Per Cent Rough Fracture Surface
6-77	547	0	2574	63.8	0.80	63.0	0.0090	0.715	100
6-95	547	0	2735	81.0	1.54	79.5	0.0170	0.894	100
6-41*	549	1.5	635	1.37	0.273	1.10	0.010	0.015	15
6-39*	551	1.75	425	2.27	0.363	1.91	0.01	0.03	10
6-37*	552	1.9	560	1.36	0.318	1.04	0.01	0.02	10
6-28*	554	2.2	225	2.89	0.99	1.90	0.02	0.035	10
6-30*	556	2.6	190	2.01	0.366	1.65	0.010	0.020	5
6-34*	558	2.9	145	2.25	0.540	1.71	0.020	0.025	10
6-36*	560	3.4	160	2.56	0.638	1.92	0.018	0.030	2
6-33*	562	3.9	245	3.64	0.638	3.00	0.010	0.040	0
6-40*	563	4.1	85	1.84	0.644	1.20	0.015	0.020	0

* - Reference 12.

Table 14. Experimental Data for the 6 Per Cent Copper Alloy Tested at a Strain Rate of 20.0 Inches Per Minute.

Specimen Number	Temp °C	Per Cent Liquid	Stress psi	Total Strain in/in x100	Strain to Max Stress in/in x100	Strain from Max Stress to Fracture in/in x100	Time to Max Stress min	Total Time min	Est. Per Cent Rough Fracture Surface
6-91	225	0	20720	44.6	15.2	29.4	0.00833	0.024	100
6-88	325	0	9830	49.3	8.96	40.3	0.00517	0.028	100
6-79	401	0	5490	63.1	9.72	53.4	0.00542	0.035	100
6-86	437	0	5360	65.0	8.57	56.4	0.00475	0.036	100
6-81	475	0	4488	82.3	9.06	73.2	0.00508	0.046	100
6-85	499	0	4291	96.8	7.20	89.6	0.00392	0.053	100
6-83	523	0	4090	97.2	8.16	89.0	0.00392	0.053	100
6-87	532	0	4265	76.0	8.11	67.9	0.00450	0.042	100
6-96	533	0	4263	93.0	9.88	83.1	0.00550	0.052	100
6-84	542	0	4020	81.5	9.18	72.3	0.00500	0.044	100
6-89	545	0	3979	91.4	8.99	82.4	0.00500	0.051	100
6-90	547	0	4107	56.6	8.31	48.3	0.00458	0.031	100

(Continued)

Table 14. Experimental Data for the 6 Per Cent Copper Alloy Tested at a Strain Rate of 20.0 Inches Per Minute. (Continued)

Specimen Number	Temp °C	Per Cent Liquid	Stress psi	Total Strain in/in x100	Strain to Max Stress in/in x100	Strain from Max Stress to Fracture in/in x100	Time to Max Stress min	Total Time min	Est Per Cent Rough Fracture Surface
6-57*	547	0	4120	68.0	9.84	58.2	0.00200	0.019	100
6-56*	548	1.5	360	5.82	1.47	4.35	0.00067	0.002	75
6-48*	548	1.5	100	1.52	0.588	0.93	0.00130	0.003	25
6-54*	549	1.5	360	5.00	1.52	3.48	0.00130	0.003	50
6-52*	549	1.5	100	1.82	1.21	0.61	0.00100	0.003	5
6-45*	549	1.5	92.5	1.71	0.60	0.61	0.00050	0.002	10
6-50*	550	1.6	147.5	3.02	1.20	1.82	0.00067	0.002	10
6-46*	551	2.2	182	5.50	1.56	3.94	0.00100	0.002	10
6-51*	554	2.2	125	5.40	1.98	3.42	0.00100	0.003	5
6-55*	560	3.4	50	3.03	1.21	1.82	0.00067	0.002	0
6-58*	565	4.8	65	4.85	1.35	3.50	0.00100	0.003	0

* = Reference 12.

APPENDIX B

THERMOCOUPLE CALIBRATION

The test thermocouples were calibrated in the range of temperatures used during the experimental investigation using a calibrated platinum-platinum ten per cent rhodium Leeds and Northrup thermocouple. A Leeds and Northrup Type K-3 Universal Potentiometer was used to record the millivolt readings of all three thermocouples. Also the same cold junction was used for all three.

The results of the calibration test (Table 15) show that the temperature readings of both the front and rear thermocouples were from 0.0 to 0.3 degrees centigrade above the temperature reading of the master thermocouple. The calibration data supplied by the manufacturer of the master thermocouple states that the uncertainty in the readings of the master thermocouple is not more than 0.75 degrees centigrade for the temperature range of 0 to 1100 degrees centigrade. This indicates that the error for both the front and rear thermocouples was between 0.0 and 1.05 degrees centigrade. The maximum possible error in the higher temperature range was about 0.3 per cent.

An additional check on the temperature measuring system was obtained by immersing the thermocouples in a mixture of ice and water and recording the temperature. The thermocouples were then immersed in boiling distilled water and the temperatures recorded. In both cases the measured temperatures and the actual temperatures did not vary by

by more than 0.1 degrees centigrade.

The test thermocouples had originally been calibrated before the tests were performed. The results of this calibration, which was made after the tests were performed, agreed with the results of the previous calibration. This indicated that the test thermocouples were not contaminated during the experimentation.

Table 15. Thermocouple Calibration Data

Thermocouple					
Master		Front		Rear	
Millivolt Reading	Temperature Degrees Centigrade	Millivolt Reading	Temperature Degrees Centigrade	Millivolt Reading	Temperature Degrees Centigrade
1.4486	201.4	1.4481	201.4	1.4490	201.4
1.6528	225.3	1.6552	225.6	1.6540	225.4
1.8782	251.2	1.8802	251.4	1.8802	251.4
2.3061	298.9	2.3084	299.2	2.3091	299.2
2.8737	360.2	2.8767	360.5	2.8764	360.5
3.1885	393.5	3.1914	393.7	3.1925	393.8
3.7243	449.2	3.7255	449.3	3.7259	449.4
3.9618	473.7	3.9638	373.9	3.9616	473.7
4.2239	500.2	4.2242	500.3	4.2255	500.4
4.2517	503.2	4.2536	503.4	4.2521	503.2
4.5461	532.8	4.5494	533.1	4.5461	532.8
4.6513	543.3	4.6545	543.6	4.6517	543.4
4.9359	571.7	4.9356	571.7	4.9376	571.9
5.2370	601.3	5.2402	601.6	5.2380	601.4
5.4030	617.5	5.4061	617.8	5.4042	617.6
5.4221	619.4	5.4215	619.4	5.4230	619.5
5.5511	631.9	5.5536	632.2	5.5527	632.1
5.5856	635.3	5.5880	635.5	5.5871	635.4

APPENDIX C

CALCULATION OF ENERGY INPUT REQUIRED TO RAISE TEMPERATURE OF FRACTURE ZONE ONE DEGREE CENTIGRADE

The following procedure was used to calculate the amount of energy required to raise five per cent of the volume of the specimen one degree centigrade.

1. The following properties of the aluminum-copper alloy were found and converted to the necessary units:

(a) Specific heat, $c_p = 0.211$ cal/gm-^oC

$= 0.840 \times 10^{-3}$ Btu/gm-^oC

(b) Density, $\rho = 174$ lbs/ft^3

$= 0.1007$ lbs/in^3

$= 45.72$ gm/in^3

(c) Volume, $V = A \times L = 0.02$ in^2 x 1.125 in

$= 0.02250$ in^3

(d) Volume of fracture zone, $v = 0.05 \times V$

$= 1.125 \times 10^{-3}$ in^3

2. The energy required to raise the volume of the fracture zone was then calculated using the above values:

Energy required, $E = c_p \times 778$ ft-lbs/Btu

$= 0.6535$ ft-lbs/gm-^oC

$= 7.84$ in-lbs/gm-^oC

$= 358.4$ in-lbs/in^3-^oC

$= 0.4032$ in-lbs/^oC

APPENDIX D

MECHANISM OF SLIP

The most common mechanism of plastic deformation in crystalline materials is slip, in which two planes of atoms slip past each other. This slip results in one whole section of the crystal (or grain) shifting relative to another section. Another mechanism of plastic deformation is twinning, where atomic movements are not whole lattice vectors. The lattice generated in the deformed region, although the same as the parent lattice, is oriented in a twin relationship to it. However, Smallman[24] states that mechanical twinning plays only a minor part in the deformation of aluminum and copper. Also, twinning seems to be governed by laws similar to those of slip and sometimes the two mechanisms are closely inter-related. Therefore this discussion will be limited to deformation by slip.

Slip occurs most easily on certain crystallographic planes, depending on the crystal structure. The planes of easy slip are those which have the largest number of atoms per unit area. In these planes the atoms are most closely spaced, and adjacent planes can slip over them easily. In the single phase region the aluminum-copper alloy system has a face-centered cubic crystalline structure. In this structure the plane of easiest slip is the (111) plane and the direction of easiest slip is the [110] direction, which is a line in the slip plane on which the atoms are most closely spaced.

Slip begins at a point in the glide plane where the presence of an imperfection makes it possible and moves through the crystal by a progressive shifting of atoms along the plane. The imperfections usually responsible for slip are called dislocations. Dislocations are small groups of atoms in the crystal lattice that are displaced from their regular positions, distorting the lattice slightly. They are present in great numbers in all crystals, having been formed during growth and by previous plastic deformation. There are two types of dislocations, the edge dislocation and the screw dislocation. In the edge dislocation the atoms are displaced at right angles to the line of the dislocation, while in the screw dislocation the atoms are displaced along the line of the dislocation. Because of the complexity of the screw dislocation only the edge dislocation will be discussed here, but it must be remembered that both edge and screw dislocations are present in the real material.

An edge dislocation occurs where a few atoms are squeezed out of place by the presence of an extra row of atoms in part of the crystal. The application of a shear stress causes a general distortion of the crystal which tends to move the extra row of atoms into a line with the bottom half of a full row of atoms. The bond between two atoms in this full row is broken, and a new bond is formed between the extra row of atoms and the lower portion of the newly broken row. Now another extra row of atoms is present, except that it is located one atomic distance from where the other extra row was originally. Thus the dislocation has shifted through one atomic distance. If the stress is maintained, the dislocation will continue to move until it reaches the edge of the crystal. The result is a general slip of one atomic distance along the

glide plane.

In a tensile specimen with a load P applied, the maximum shear stress always acts on any plane making an angle of 45° with the axis of the applied stress and is equal to one half the applied stress. When a face-centered cubic crystal is oriented so that the (111) plane is at an angle of 45° to the axis of the applied stress, the maximum shearing stress acts along these planes of easiest slip. The effect of the shearing stress is to shift these planes of atoms relative to each other by causing movement of the dislocations present. When the applied stress reaches the value at which yielding begins, a dislocation moves progressively along the plane until the entire plane of atoms has shifted relative to the plane of atoms adjacent to it. This process continues as the movement of more dislocations allows additional layers of atoms to slip past each other, and the crystal continues to lengthen.

Normally the slip planes in a single crystal do not coincide with the plane of maximum shear. Because of this, it is necessary to determine the shearing stress on a given potential slip plane, and from that, its component in the direction of easy slip. The stress in this direction of easy slip is called the resolved shear stress, and the stress at which slip begins on this particular plane is the critical resolved shear stress. A derivation of the resolved shear stress is given in Figure 32. The magnitude of the resolved shear stress depends on the orientation of the slip plane with reference to the direction of loading, but it will always be less than or equal to the maximum shear stress. For the resolved shear stress to become critical, that is, to cause slip to begin, a tensile stress larger than that requred for slip

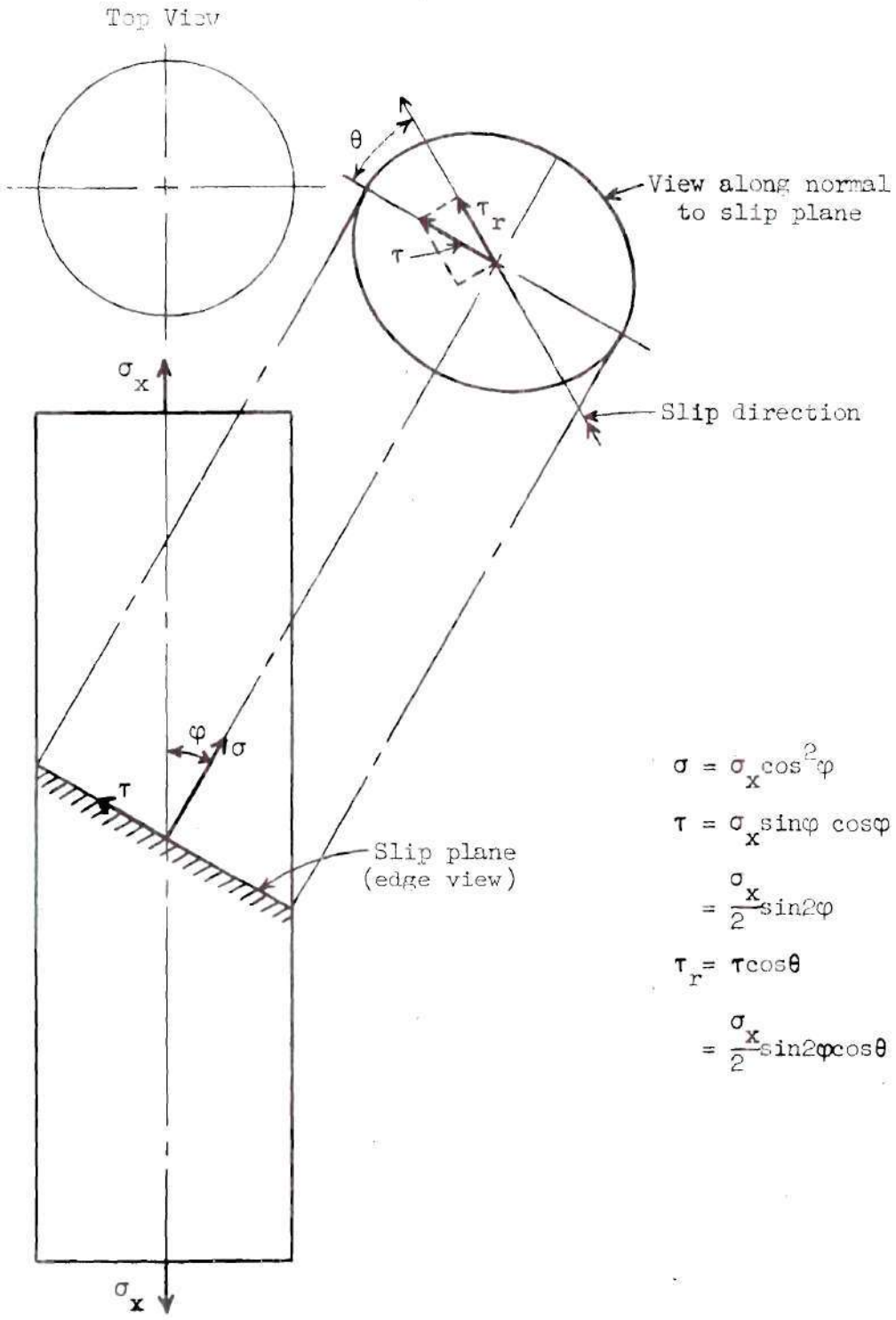

Figure 32. Derivation of Resolved Shear Stress.

if the plane of easiest slip is at an angle of 45° to the axis of the stress will be required. The plane on which slip will first take place will be that one most favorably oriented and having the highest resolved shear stress.

LITERATURE CITED

1. A. R. E. Singer and P. H. Jennings, "Hot-Shortness of the Aluminum-Silicon Alloys of Commercial Purity," Journal Institute of Metals, 1946, 73, 197.

2. P. H. Jennings, A. R. E. Singer, and W. I. Pumphrey, "Hot-Shortness of Some High-Purity Alloys in the Systems Aluminum-Copper-Silicon and Aluminum-Magnesium-Silicon," Journal Institute of Metals, 1948, 74, 227.

3. N. N. Prokhorov, "Resistance to Hot Tearing of Cast Metals During Solidification," Russian Castings Production, April 1962, 172.

4. R. Eborall and P. Gregory, "The Mechanism of Embrittlement by a Liquid Phase," Journal Institute of Metals, 1955-56, 84, 88.

5. A. A. Griffith, "The Phenomena of Rupture and Flow in Solids," Philosophical Transactions of the Royal Society, 1920 (A) 221, 163.

6. C. S. Smith, "Grains, Phases, and Interfaces: An Interpretation of Microstructure," Transactions American Institute of Metallurgical Engineers, 175, 1948, 15.

7. J. Vero, "Hot Shortness of Aluminum Alloys," Metal Industry, 1936, 48, 431, 491.

8. A. R. E. Singer and S. A. Cottrell, "Properties of the Aluminum-Silicon Alloys at Temperatures in the Region of the Solidus," Journal Institute of Metals, 1947, 73, 33.

9. W. I. Pumphrey and P. H. Jennings, "High-Temperature Tensile Properties of Cast Aluminum-Silicon Alloys and Their Constitutional Significance," Journal Institute of Metals, 1948, 75, 203.

10. J. V. Lyons and W. I. Pumphrey, "The Properties of Some Binary Aluminum Alloys at Elevated Temperatures," Metallurgia, 45-56, 1952, 219, 299.

11. I. I. Novikov, "Alloying Non-Ferrous Alloys to Reduce Hot Brittleness," Russian Castings Production, April 1962, 167.

12. T. F. Talbot, "Deformation of Some Aluminum-Copper Alloys in the Region of the Solidus," Ph.D. Thesis, Georgia Institute of Technology, June 1964.

13. A. Nadai and M. J. Manjoine, "High Speed Tension Tests at Elevated Temperatures - Parts II and III," Journal of Applied Mechanics, June 1941, A-77.

14. W. S. Pellini, "Strain Theory of Hot Tearing," Foundry, November 1952, 132.

15. A. R. E. Singer and P. H. Jennings, "Hot-Shortness of Some Aluminum-Iron-Silicon Alloys of High Purity," Journal Institute of Metals, 1947, 73, 273.

16. J. C. Borland, "Generalized Theory of Super-Solidus Cracking in Welds (and Castings)," British Welding Journal, 1960, 8, 508.

17. V. N. Saveiko, "Theory of Hot Tearing," Russian Castings Production, 1961, 453.

18. W. Patterson, "Mechanism of Hot Tear Formation in Casting Alloys," Giesserie, (Techn. Wise. Beihafte) 12, 1953, 597.

19. Y. A. Smolyanitsky, "The Criterion for Hot-Shortness in Alloys," Invest. Vus. Chern. Met., (2), 1960, 124.

20. N. N. Prokhorov, "Ductility of Solidifying Metals," Russian Castings Production, April 1962, 176.

21. J. H. Tundermann, "A Study of the Effects of Temperature on the Dihedral Angles and Interface Energies of Some Ternary Al-Sn-Cu, Sb, Si, Li, Mg, and In Alloys," Master's Thesis, Georgia Institute of Technology, December, 1964.

22. C. W. Richards, "Engineering Materials Science," 1961, Wadsworth, 83, 283.

23. G. E. Dieter, Jr., "Physical Metallurgy," 1961, McGraw-Hill, 248-250.

24. R. R. Smallman, "Modern Physical Metallurgy," 1962, Butterworth and Company, 154.

25. D. McLean, "Mechanical Properties of Metals," 1962, Wiley and Sons, 303, 307.

26. A. G. Guy, "Elements of Physical Metallurgy," 1960, Addison-Wesley, 316.